New Results on Charm Spectroscopy in LHCb.

Antimo Palano

INFN and University of Bari, Italy

JLAB

From the LHCb Collaboration

Outline:

- New results on charm spectroscopy.
- Results on strange charm spectroscopy.

Jefferson LAB, March 28, 2014

Spectroscopy

□ In the last years we have observed an increasing interest in spectroscopy.

□ BaBar, Belle, BES, COMPASS, LHCb, CMS, and ATLAS experiments are very active in producing new results on spectroscopy an search for “exotic” particles.

□ There are observations of multiquark states candidates, charged charmonium and bottomonium resonances, hybrid states ...

□ However the quest of the existence of gluonium states still remain to be solved.

Spectroscopy

□ The new interest in spectroscopy started in 2003 with the discovery by BaBar of the unexpected narrow $D^*_{s0}(2317) \to D_s \pi^0$ resonance.

□ Recent SPIRES check: the number of citations of the $D^*_{s0}(2317)$ paper is similar to that of the observation of CP violation in B^0 decays!

Observation of CP violation in the B^0 meson system
BaBar Collaboration (Bernard Aubert (Annecy, LAPTH) *et al.*). Jul 2001. 8 pp.
Published in **Phys.Rev.Lett. 87 (2001) 091801**
SLAC-PUB-8904, BABAR-PUB-01-18
DOI: 10.1103/PhysRevLett.87.091801
e-Print: **hep-ex/0107013** | **PDF**
References | BibTeX | LaTeX(US) | LaTeX(EU) | Harvmac | EndNote
ADS Abstract Service; BaBar Publications Database; BaBar Password Pr
Detailed record - Cited by 662 records 500+

Observation of a narrow meson decaying to $D_s^+ \pi^0$ at a mass of 2.32-GeV/c^2
BaBar Collaboration (B. Aubert (Annecy, LAPP) *et al.*). Apr 2003. 7 pp.
Published in **Phys.Rev.Lett. 90 (2003) 242001**
SLAC-PUB-9711, BABAR-PUB-03-011
DOI: 10.1103/PhysRevLett.90.242001
e-Print: **hep-ex/0304021** | **PDF**
References | BibTeX | LaTeX(US) | LaTeX(EU) | Harvmac | EndNote
CERN Document Server ; ADS Abstract Service; BaBar Publications Database; Bal
Detailed record - Cited by 657 records 500+

Charm meson spectroscopy

□ The quark model predicts many states with different quantum numbers in limited mass regions (Godfrey and Isgur, Phys.Rev.D32,189 (1985)).

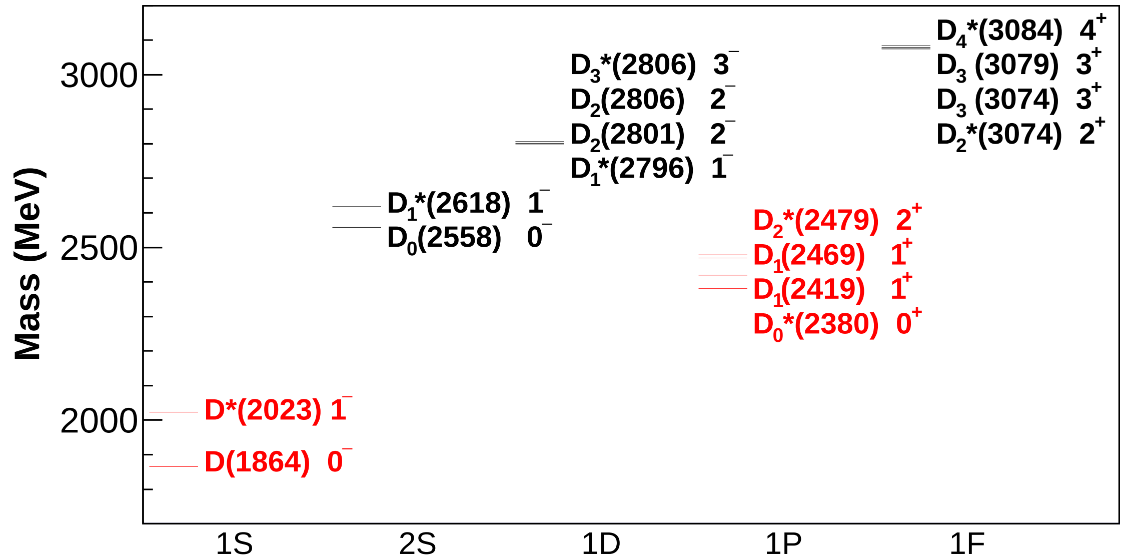

□ In red are shown the established states.

□ The ground states (D, D^*), and two of the 1P states, $D_1(2420)$ and $D_2^*(2460)$, are experimentally well established since they have relatively narrow widths (∼30 MeV).

Charm meson spectroscopy

- Masses (in GeV) of charmed meson computed by Godfrey and Isgur.
- For a $Q\bar{q}$ system, L: orbital angular momentum between Q and $\bar{q}$, $j = L + s_{\bar{q}}$.

$c\bar{q}$ $(L=0)$	Mass	$c\bar{q}$ $(L=1)$	Mass	$c\bar{q}$ $(L=2)$	Mass
$D(^1S_0)$	1.88	$D(^3P_0)$	2.40	$D(^3D_1)$	2.82
$D(^3S_1)$	2.04	$D(^3P_1)$	2.49	$D(^3D_3)$	2.83
		$D(^3P_2)$	2.50		
		$D(^1P_1)$	2.44		

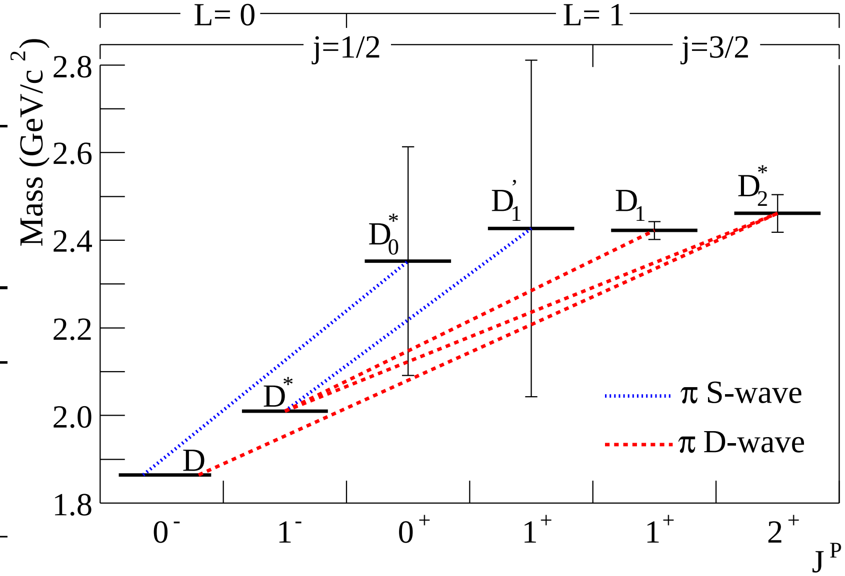

- Properties of neutral $L = 1$ D_J mesons.

	J^P	Mass (MeV)	Width (MeV)	*Decays*
D_0^*	0^+	2318 ± 29	267 ± 40	$D\pi$
D_1'	1^+	2427 ± 26	384^{+107}_{-75}	$D^*\pi$
D_1	1^+	2421.3 ± 0.6	27.1 ± 2.7	$D^*\pi, D^0\pi^+\pi^-$
D_2^*	2^+	2462.6 ± 0.7	49.0 ± 1.4	$D^*\pi, D\pi$

- Broad states difficult to establish experimentally.

Observation of $D_0^*(2400)$

□ The broad $L = 1$ states, $D_0^*(2400)$ has been established by the Belle and BaBar experiments in a Dalitz analysis of $B^+ \to D^- \pi^+ \pi^+$ (hep-ex/0307021,arXiv:0901.1291v2).

□ Data from BaBar.

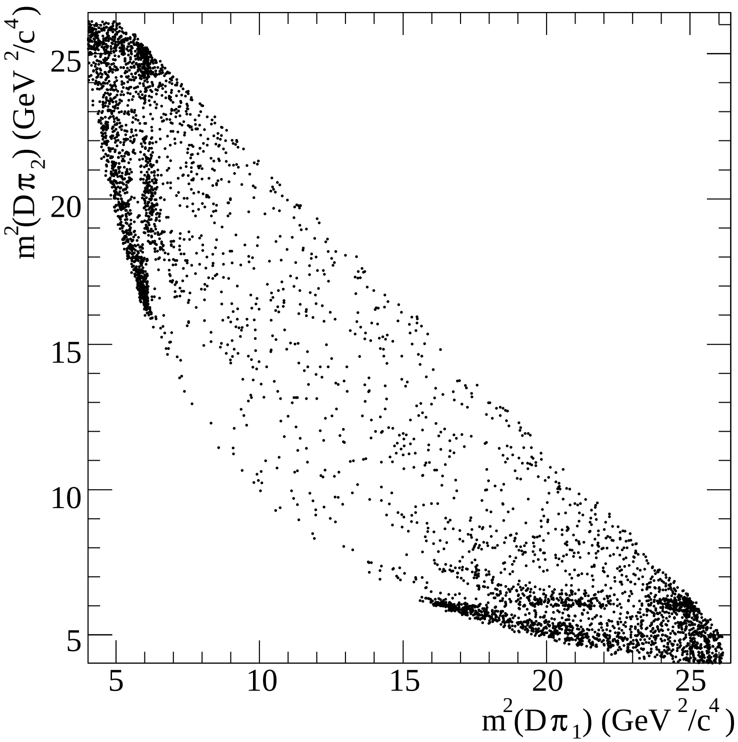

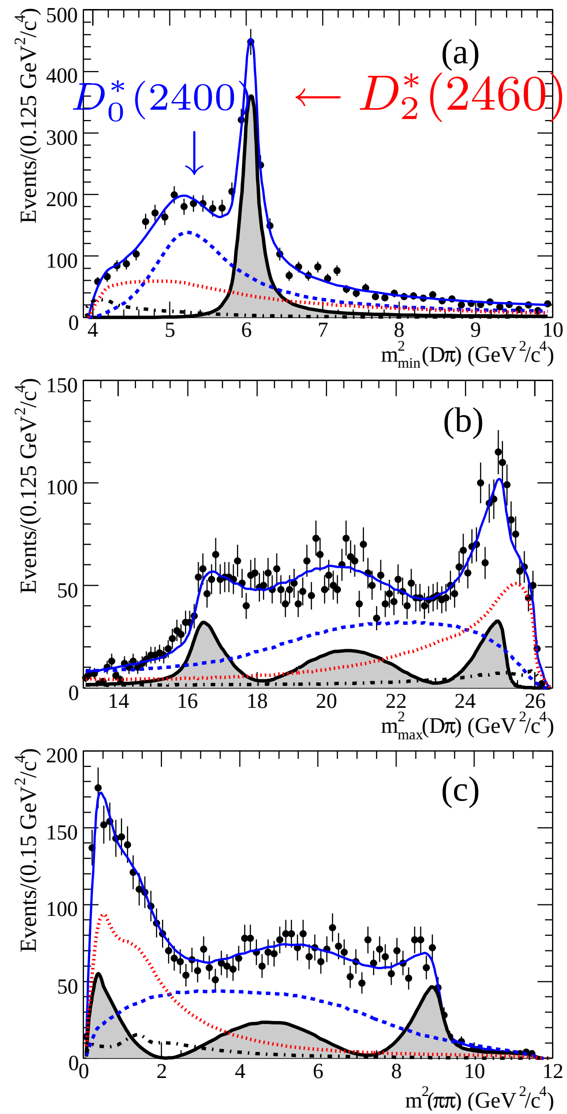

$$m_{D_0^{*0}} = (2297 \pm 8 \pm 5 \pm 19)\,\mathrm{MeV}/c^2,\ \Gamma_{D_0^{*0}} = (273 \pm 12 \pm 17 \pm 45)\ MeV.$$

Observation of $D_1'(2430)$

□ The $D_1'(2430)$ has been been observed by Belle in a Dalitz analysis of $B^+ \to D^{*-}\pi^+\pi^+$ decays (hep-ex/0307021)

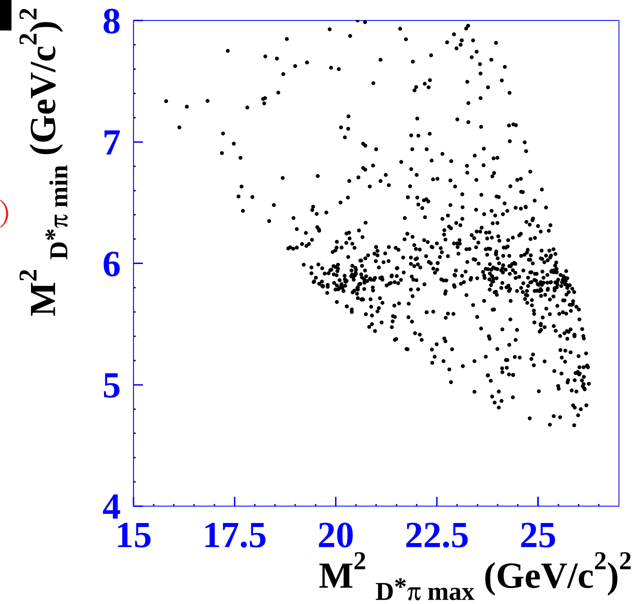

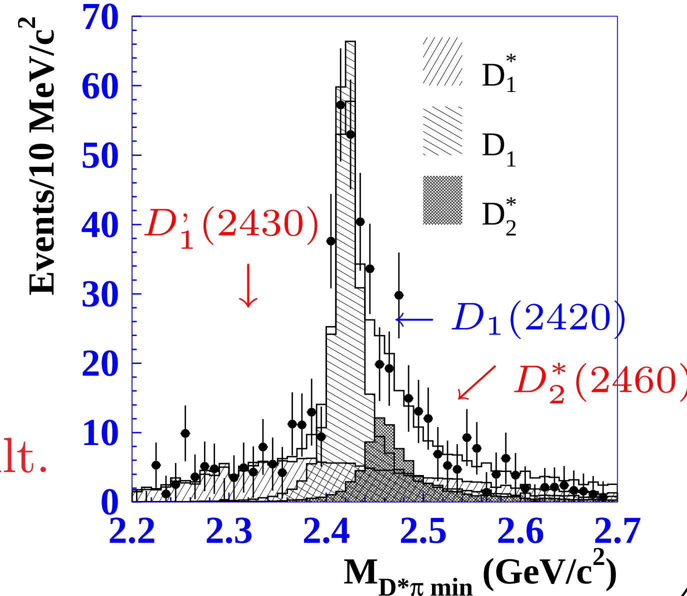

$$M_{D_1'^0} = (2427 \pm 26 \pm 20 \pm 15)\,\mathrm{MeV}/c^2$$

$$\Gamma_{D_1'^0} = (384^{+107}_{-75} \pm 24 \pm 70)\,\mathrm{MeV}$$

□ Low statistics analysis. LHCb should improve this result.

Recent results from BaBar.

☐ Study of the $D^+\pi^-$, $D^0\pi^+$, and $D^{*+}\pi^-$ final states in the reaction $e^+e^- \rightarrow c\bar{c} \rightarrow D^{(*)}\pi X$

(Phys.Rev.D82,111101(2010)).

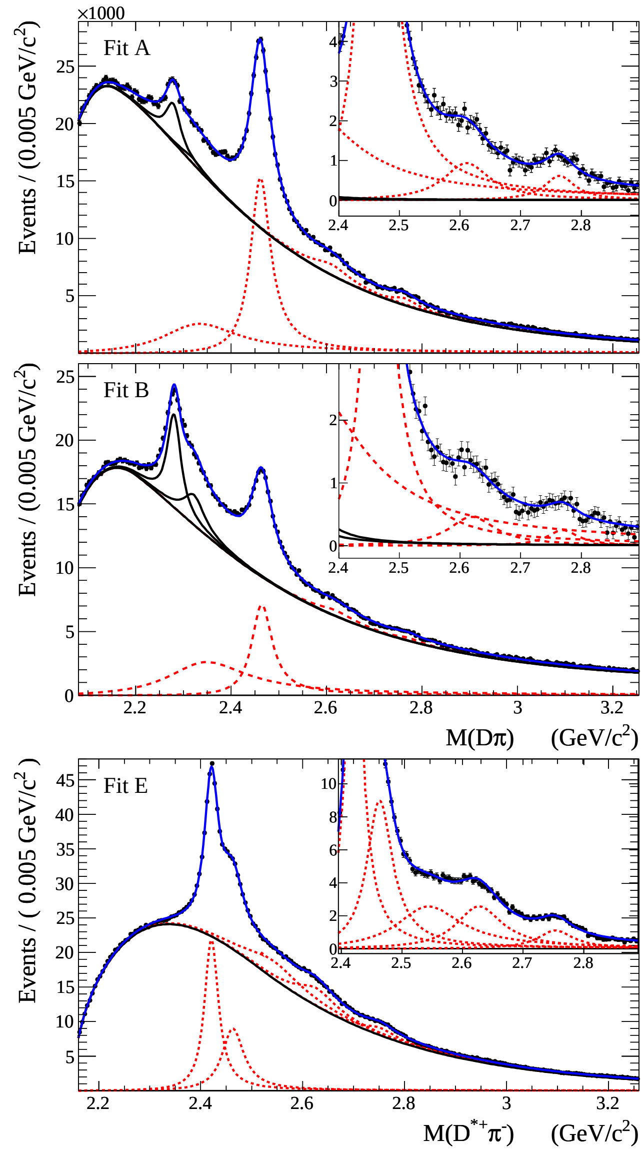

☐ *Observed four new states decaying to $D\pi$ and $D^*\pi$:*

$D_J(2580)^0$, $D^*_J(2650)^0$, $D_J(2740)^0$, and $D^*_J(2760)^0$.

☐ Performed a spin-parity analysis.

☐ **Very complex experimental environment which require confirmation.**

The LHCb experiment.

□ LHCb experiment is collecting very large samples of $c\bar{c}$ and $b\bar{b}$ events.

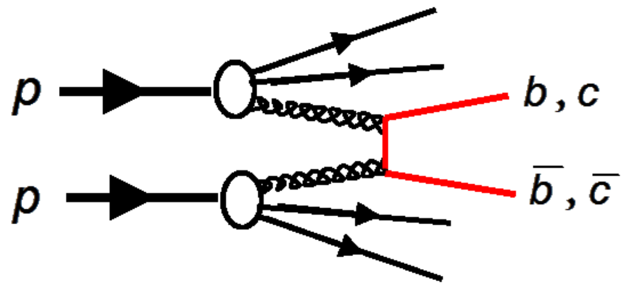

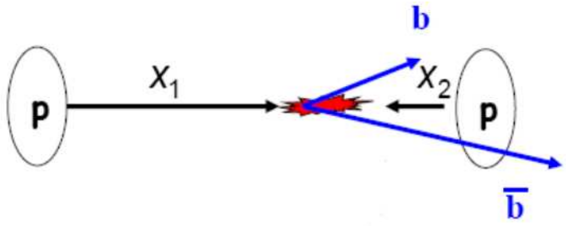

$\sigma(b\bar{b}) \quad at\ 7\ TeV\ \approx 290\ \mu b$

$\sigma(c\bar{c}) \approx 20 \times \sigma(b\bar{b})$

□ Charmed events candidates are strongly suppressed by the trigger. Except for a few channels of interest.

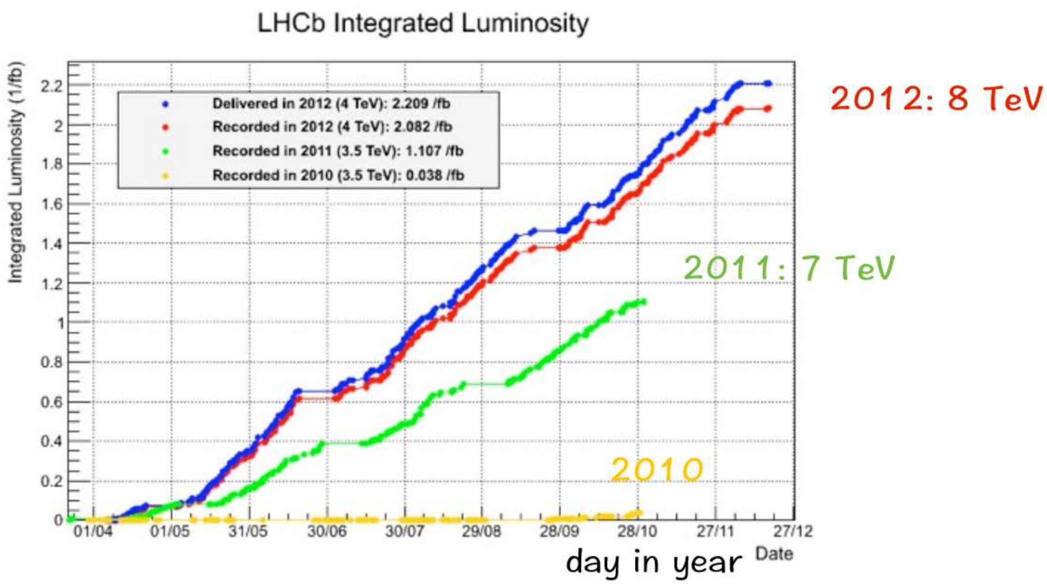

□ Collected $\approx 3.2\ fb^{-1}$.

The LHCb experiment.

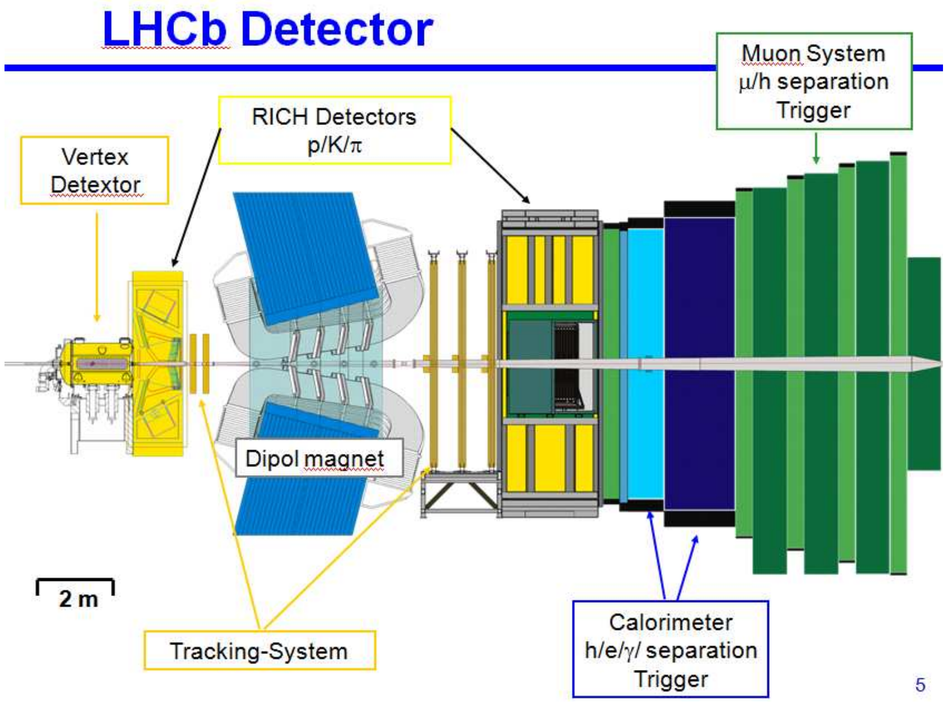

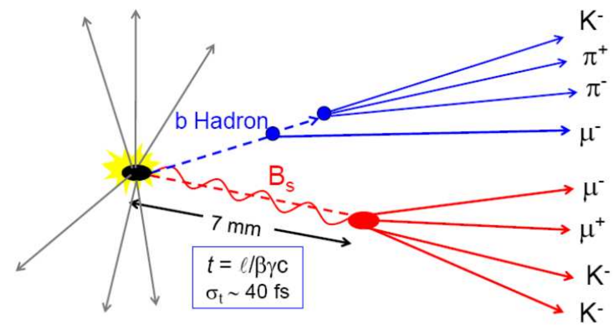

□ Precise reconstruction of primary and secondary vertices (resolution = 45 fs for $B_s \rightarrow J/\psi\phi$).

□ Excellent K/π separation (K identification efficiency = 95% with 5% of pion misidentification).

□ All type of B hadrons produced:($B^{\pm}$, B^0, B_s^0, b-baryons, $B_c^{\pm}$).

□ Main issue for B and charm physics is the large vertex separation. Big boost, long-lived particles fly over long distances. Easy secondary vertex separation.

Study of the $D\pi$ and $\pi^- D^{*+}$ systems in LHCb

□ We reconstruct the following final states (arXiv:1307.4556):

$$\mathbf{pp} \rightarrow \mathbf{X} \quad \pi^- \mathbf{D}^+$$
$$\rightarrow K^-\pi^+\pi^+$$

$$\mathbf{pp} \rightarrow \mathbf{X} \quad \pi^+ \mathbf{D}^0$$
$$\rightarrow K^-\pi^+$$

$$\mathbf{pp} \rightarrow \mathbf{X} \quad \pi^- \mathbf{D}^{*+}$$
$$\rightarrow \pi^+ D^0$$
$$\rightarrow K^-\pi^+$$

at 7 TeV, where **X** represents any collection of charged and neutral particles.

□ The analysis based on ($\approx 1\ fb^{-1}$) of data.

□ D^+, D^0, and D^{*+} signals.

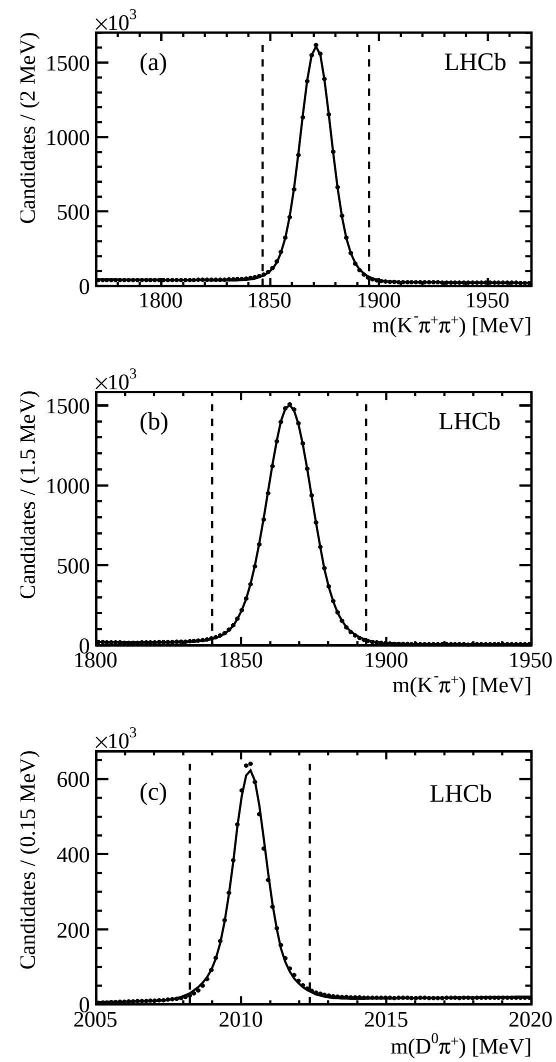

The use of charge-conjugate decay modes is implied.

Data selection.

□ Reconstructed D and D^* are combined with another hadron pointing to the same primary vertex.

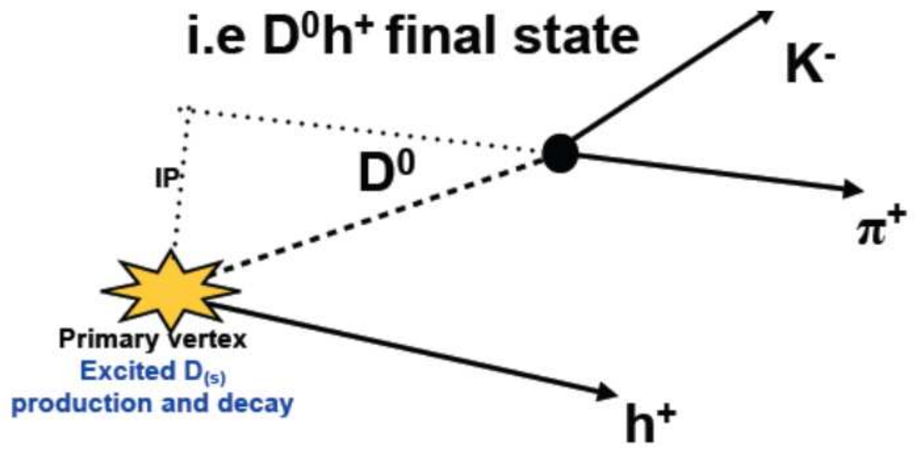

□ However a large combinatorial problem: events can have more than 100 tracks.

□ A limited events pile-up is also present.

The $cos\theta$ cut.

☐ Combinatorial issues are strongly reduced by the use of the angle θ.

☐ *For a $D^*\pi$ system, θ is the angle formed by the π in the $D^*\pi$ rest frame with the $D^*\pi$ direction in the Lab. frame.*

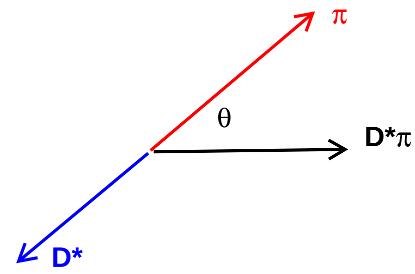

☐ For an unpolarized two-body decay of a resonance, we expect the $cos\theta$ distribution to be symmetric.

☐ Combinatorial background concentrates at $cos\theta < 0$. **Require** $cos\theta > 0$.

☐ Example from the $D^*\pi$ final state.

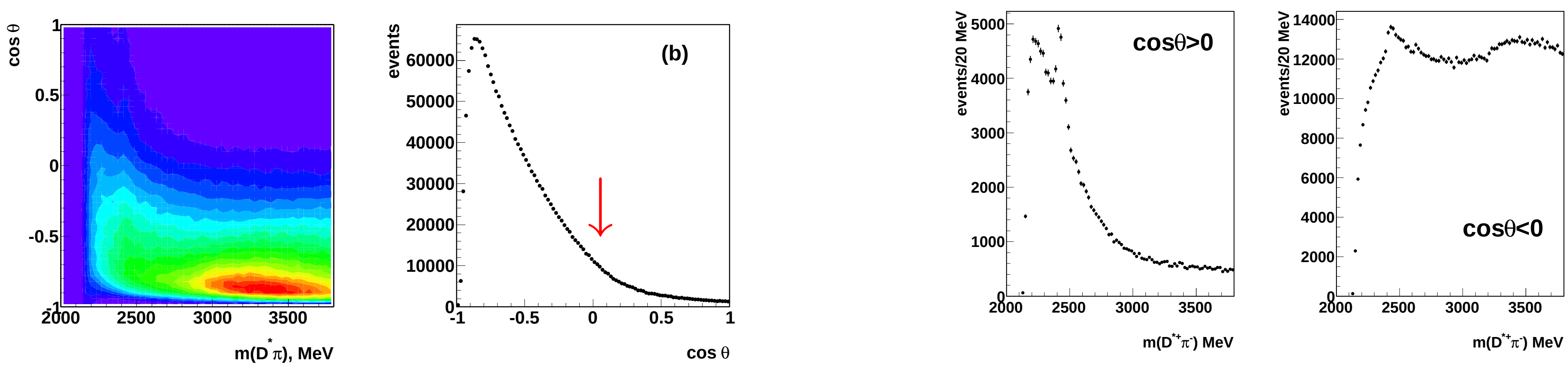

☐ **Signal to background for known resonances largely increases in the** $cos\theta > 0$ **region.**

Optimization.

- □ Signal/background ratio for the observed resonances improves with $p_T(D^{(*)}\pi)$.
- □ For the $D^+\pi^-$ mass spectrum we optimize on the strong $D_2^*(2460)^0$ signal.
- □ Fit the $D^+\pi^-$ mass spectrum with increasing p_T cut.
- □ Compute:

$$Purity(P) = Signal/(Signal + Background),$$

$$Significance(S) = Signal/\sqrt{Signal + Background},$$

$$Product: \ S \cdot P$$

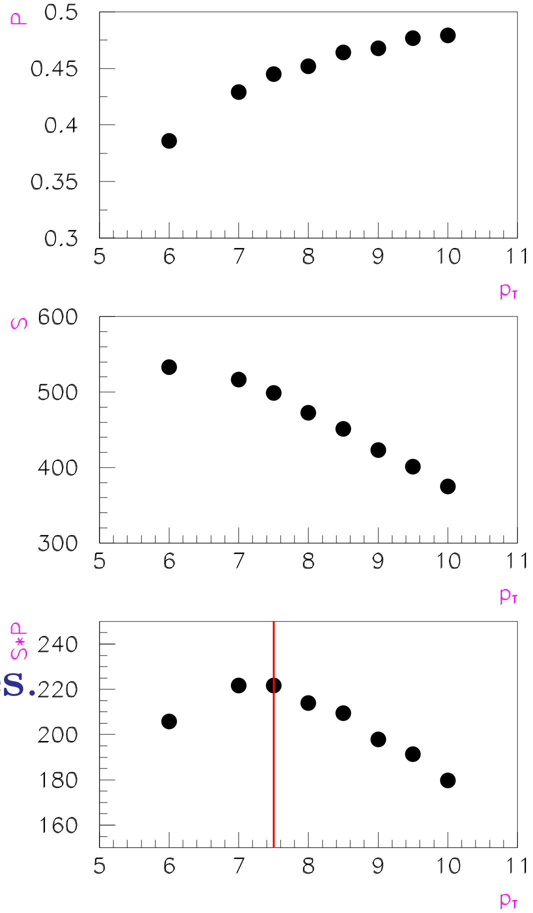

- □ **Choose a cut at $p_T > 7.5$ GeV/c for all final states.**
- □ After the optimization 7.9×10^6, 7.5×10^6 and 2.1×10^6 $D^+\pi^-$, $D^0\pi^+$ and $D^{*+}\pi^-$ candidates are obtained.

Experimental resolution and efficiency

□ Using MC simulations, we obtain mass resolution ≈ 4 MeV at the $D_2^*(2460)$ mass similar for all the channels.

□ Resolution effects negligible when compared to the widths of the resonances under study.

□ The $D^{*+}\pi^-$ final state gives information on the spin-parity assignment of a given resonance.

□ In the rest frame of the $D^{*+}\pi^-$, we define the helicity angle θ_H as the angle between the π^- and the π^+ from the D^{*+} decay.

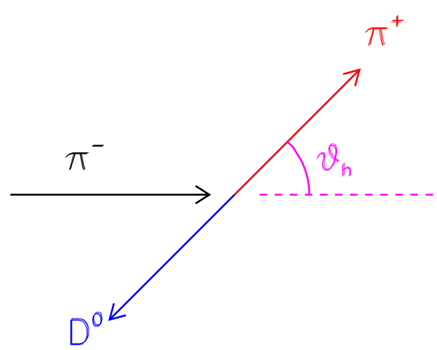

□ We compute the efficiency as a function of the helicity angle θ_H and find it uniform.

$D^+\pi^-$ and $D^+\pi^+$ mass spectra.

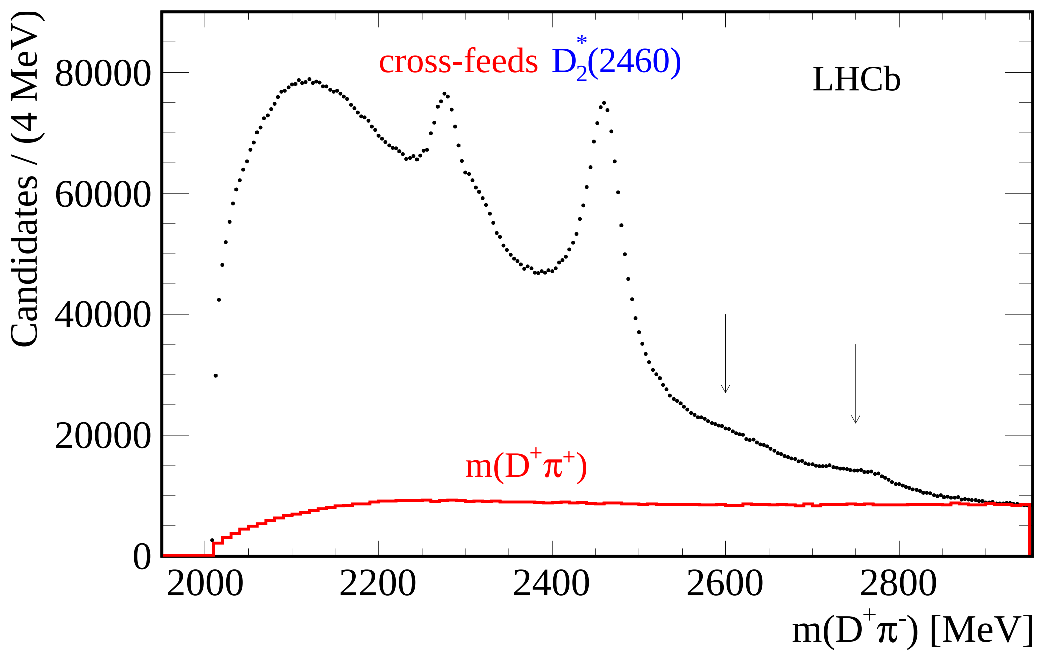

- The $D^+\pi^-$ mass spectrum shows a cross-feed from the decay

$$D_1(2420)^0 \text{ or } D_2^*(2460)^0 \to \pi^- D^{*+}(\to D^+\pi^0/\gamma) \ (32.3\%)$$

  where the π^0/γ is not reconstructed.

- Strong $D_2^*(2460)^0$ signal and weak structures around 2600 and 2750 MeV.
- The wrong-sign $D^+\pi^+$ mass spectrum does not show any structure.

$D^0\pi^+$ and $D^0\pi^-$ mass spectra.

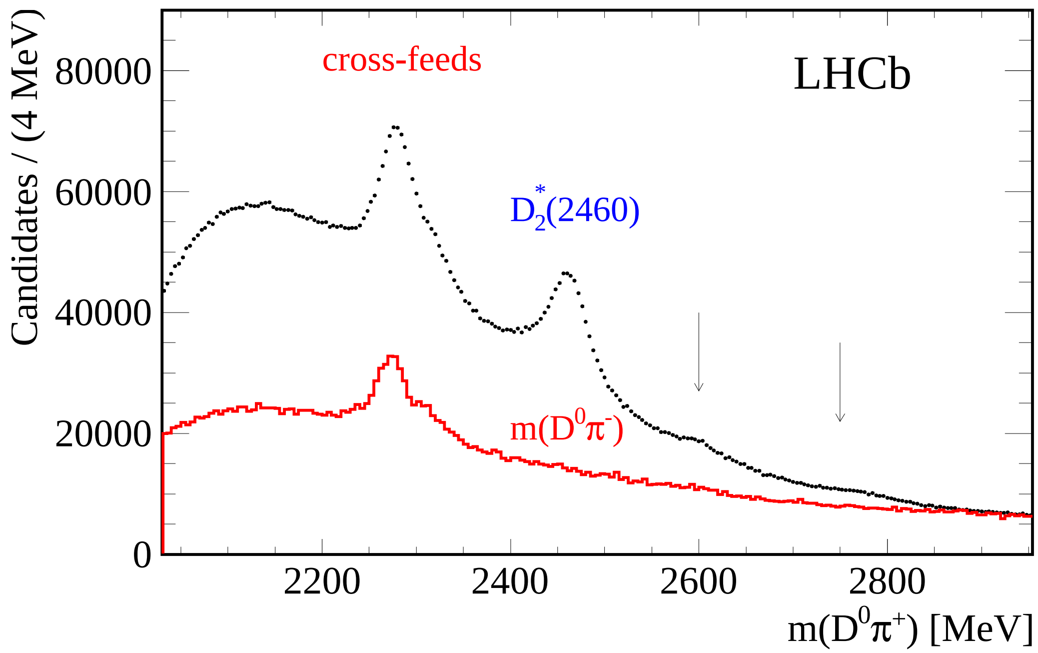

- The $D^0\pi^+$ mass spectrum shows a cross-feed from the decays:

$$D_1(2420)^+ \text{ or } D_2^*(2460)^+ \rightarrow \pi^+ D^{*0} \quad (\rightarrow D^0\pi^0) \ (61.9\%)$$

$$(\rightarrow D^0\gamma) \ (38.1\%) \ .$$

- Strong $D_2^*(2460)^+$ signal and weak structures around 2600 and 2750 MeV.
- The wrong-sign $D^0\pi^-$ mass spectrum shows cross-feeds from:

$$D_1(2420)^0 \text{ or } D_2^*(2460)^0 \rightarrow \pi^- D^{*+}(\rightarrow D^0\pi^+) \ (67.7\%)$$

$D^{*+}\pi^-$ and the $D^{*+}\pi^+$ mass spectra.

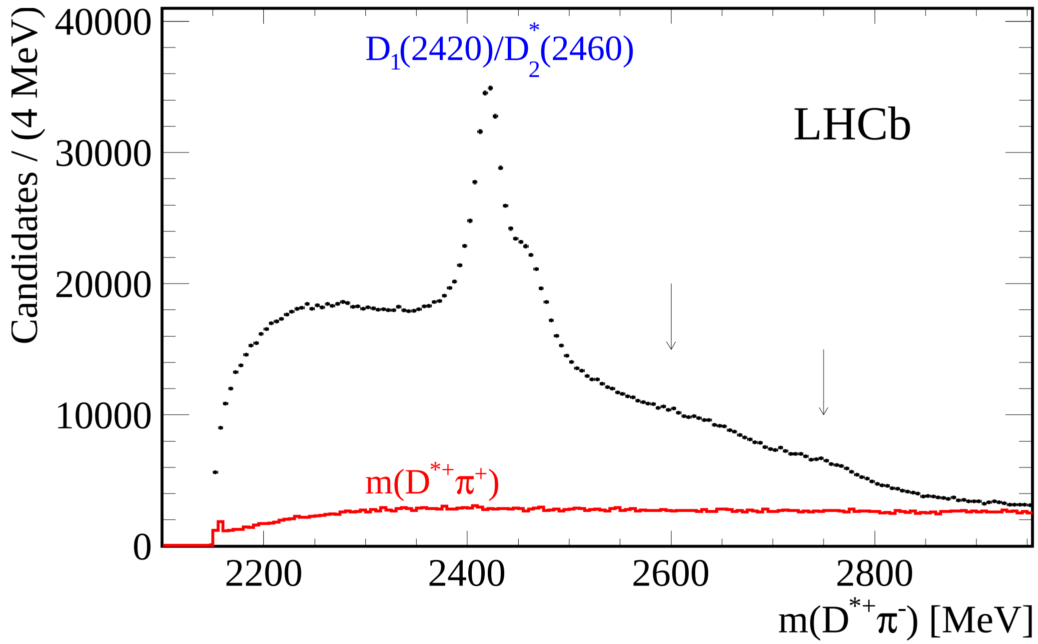

- The $D^{*+}\pi^-$ mass spectrum is dominated by the presence of the $D_1(2420)^0$ and $D_2^*(2460)^0$ signals.
- At higher mass, complex broad structures in the mass region between 2500 and 2800 MeV.
- The wrong-sign $D^{*+}\pi^+$ mass spectrum does not show any structure.
- No cross-feeds in this final state.

Study of the $D^{*+}\pi^-$ angular distributions.

□ Expected angular distributions for different spin assignments and MC simulations.

J^P	Helicity Distribution
0^+	decay not allowed
1^-	$\propto \sin^2\theta_H$
2^+	$\propto \sin^2\theta_H$
3^-	$\propto \sin^2\theta_H$
0^-	$\propto \cos^2\theta_H$
1^+	$\propto 1 + h\cos^2\theta_H$
2^-	$\propto 1 + h\cos^2\theta_H$

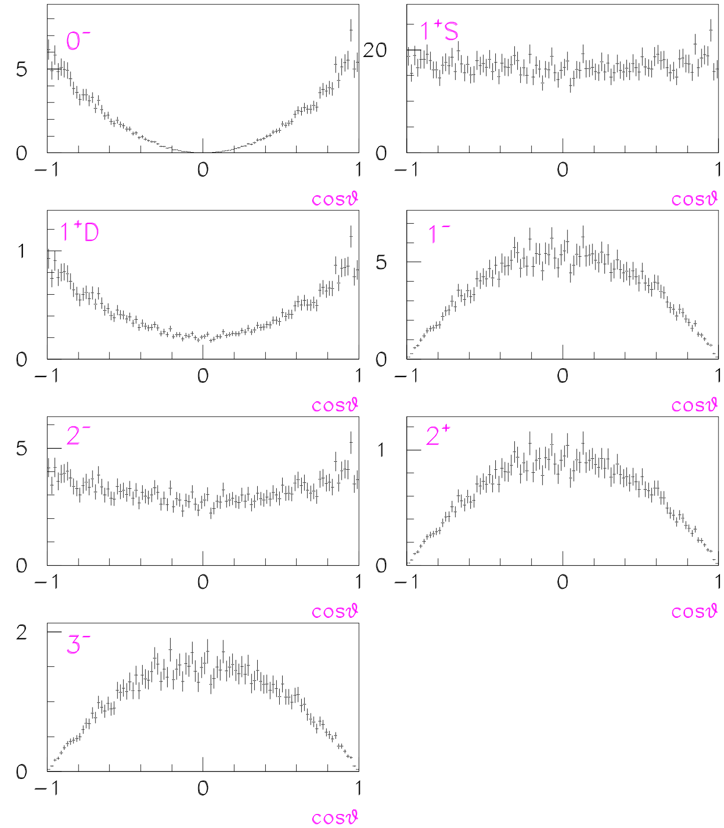

□ States having $J^P = 0^+, 1^-, 2^+, 3^-, ..$ are defined as having "Natural Parity".

□ States having $J^P = 0^-, 1^+, 2^-, ...$ are defined as having "Unnatural Parity".

□ A resonance decaying to $D\pi$ has "Natural Parity". Labelled with D^*.

Analysis strategy.

□ We have to discriminate between "true" resonances and cross-feeds.

□ The $D^{*+}\pi^-$ mass spectrum is free from cross-feeds. However it can contain both Natural Parity and Unnatural Parity resonances.

□ We make use of the angular information to produce enriched samples of Natural Parity or Unnatural Parity contributions.

□ We use the results from the $D^{*+}\pi^-$ analysis to predict cross-feeds into the $D\pi$ mass spectra.

□ We fit the $D\pi$ mass spectra searching for the Natural Parity resonances only.

□ *Slightly different strategy in BaBar: Natural Parity resonances extracted from the $D\pi$ mass spectra and fixed in the analysis of the $D^*\pi$ mass spectrum.*

Study of the $D^{*+}\pi^-$ angular distributions.

□ We divide the data into three samples:

$|\cos\theta_H| > 0.75$, **Enhanced Unnatural Parity Sample.**
(0.55×10^6 events,
Natural Parity suppressed by a factor 11.6)

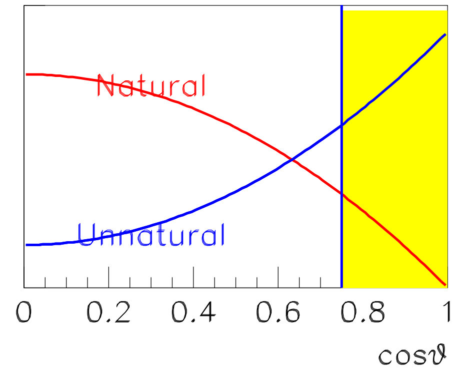

$|\cos\theta_H| < 0.5$, **Natural Parity Sample.**
(0.98×10^6 events,
Natural Parity suppressed by a factor 1.5)

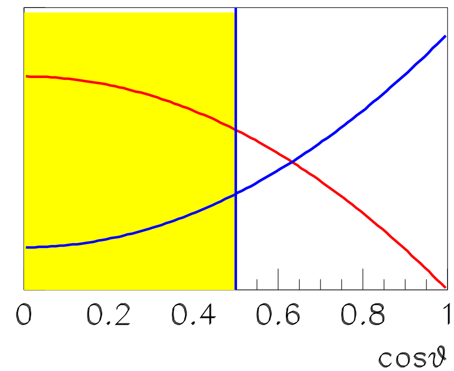

$|\cos\theta_H| > 0.5$, **Unnatural Parity Sample.**
(1.06×10^6 events,
Natural Parity suppressed by a factor 3.2)

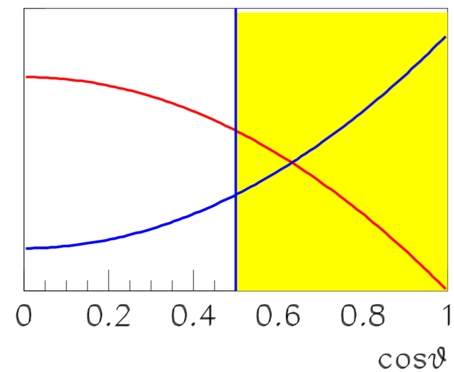

Fitting model.

□ Background model:

$$B(m) = P(m)e^{a_1 m + a_2 m^2} \; for \; m < m_0$$

$$B(m) = P(m)e^{b_0 + b_1 m + b_2 m^2} \; for \; m > m_0$$

where $P(m)$ is the two-body phase space.

b_0 and b_1 are obtained by imposing continuity on the function and its first derivative.

□ Use relativistic Breit-Wigner for $D_2^*(2460)$ and $D_0^*(2400)$ decaying to $D\pi$.

□ Simple Breit-Wigner are used for the other structures.

□ Each Breit-Wigner is multiplied by the phase-space factor.

□ The cross-feed lineshapes from $D_1(2420)$ and $D_2^*(2460)$ appearing in the $D^+\pi^-$ and $D^0\pi^+$ mass spectra are described by a Breit-Wigner function fitted to the data.

Fit to the *Enhanced Unnatural Parity Sample.*

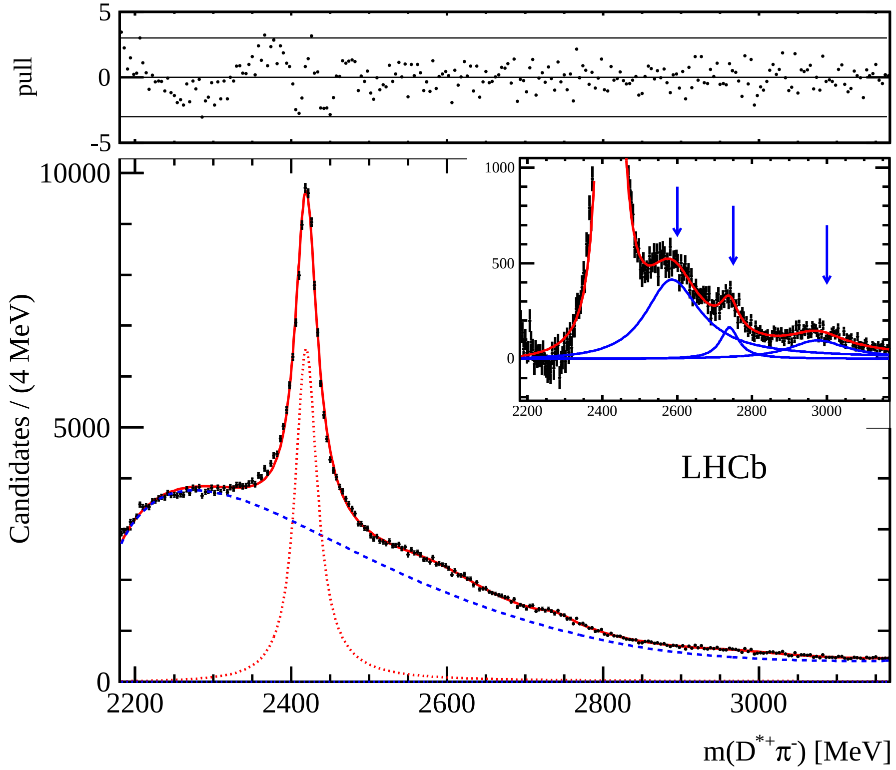

- We expect Natural Parity consistent with zero.
- $D_2^*(2460)^0$ yield consistent with zero.
- Observe $D_1(2420)^0$.
- **Observe three further structures:**

$$D_J(2580)^0, D_J(2740)^0, D_J(3000)^0$$

Fit to the *Natural Parity Sample*.

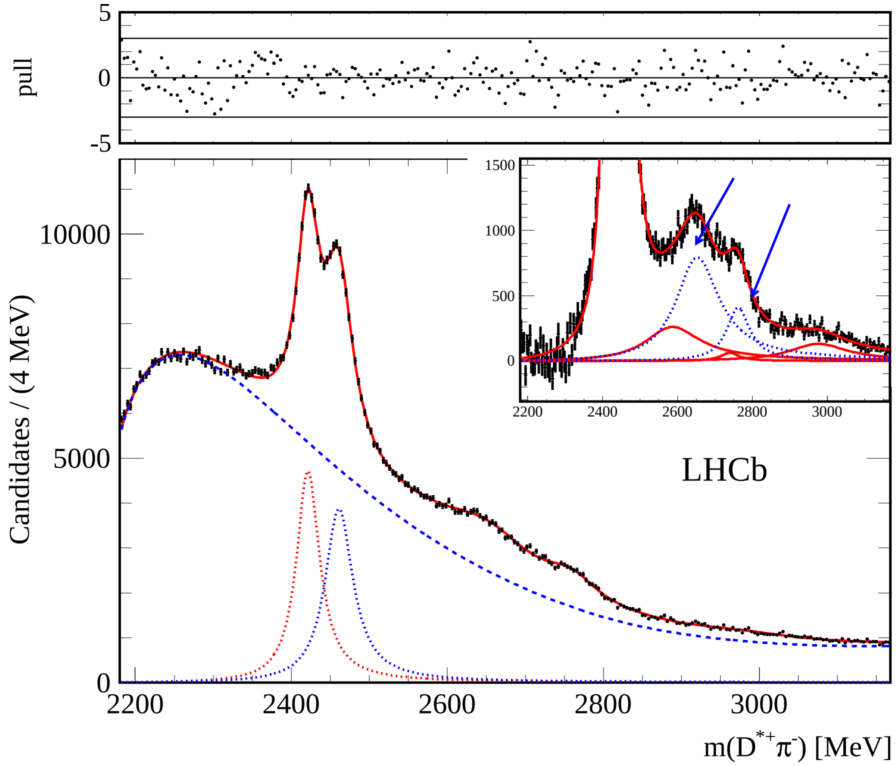

- □ We expect Enhanced Natural Parity contributions.
- □ Observe $D_1(2420)^0$ and $D_2^*(2460)^0$.
- □ Fix the $D_J(2580)^0$, $D_J(2740)^0$, and $D_J(3000)^0$ parameters.
- □ **Observe two further structures:**

$$D_J^*(2650)^0, D_J^*(2760)^0$$

Fit to the *Unnatural Parity Sample* and *Total Sample*.

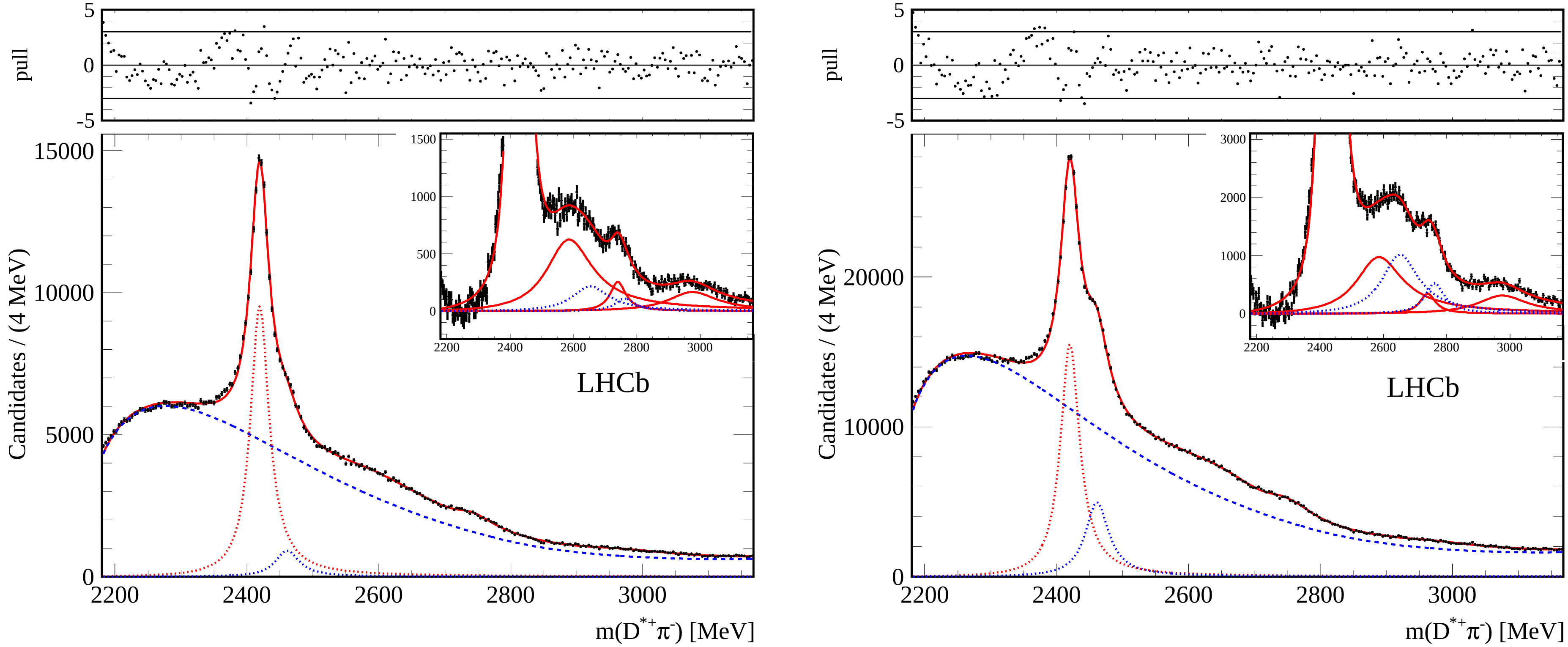

- □ Unnatural Parity Sample: fix all resonances parameters except for $D_1(2420)^0$.
- □ Total: all resonances parameters fixed.

Angular distributions.

- ◻ Divide the $D^{*+}\pi^{-}$ sample into 10 equally-spaced $cos\theta_H$ slices.
- ◻ Fit the mass spectra with fixed resonances parameters. Obtain yields.

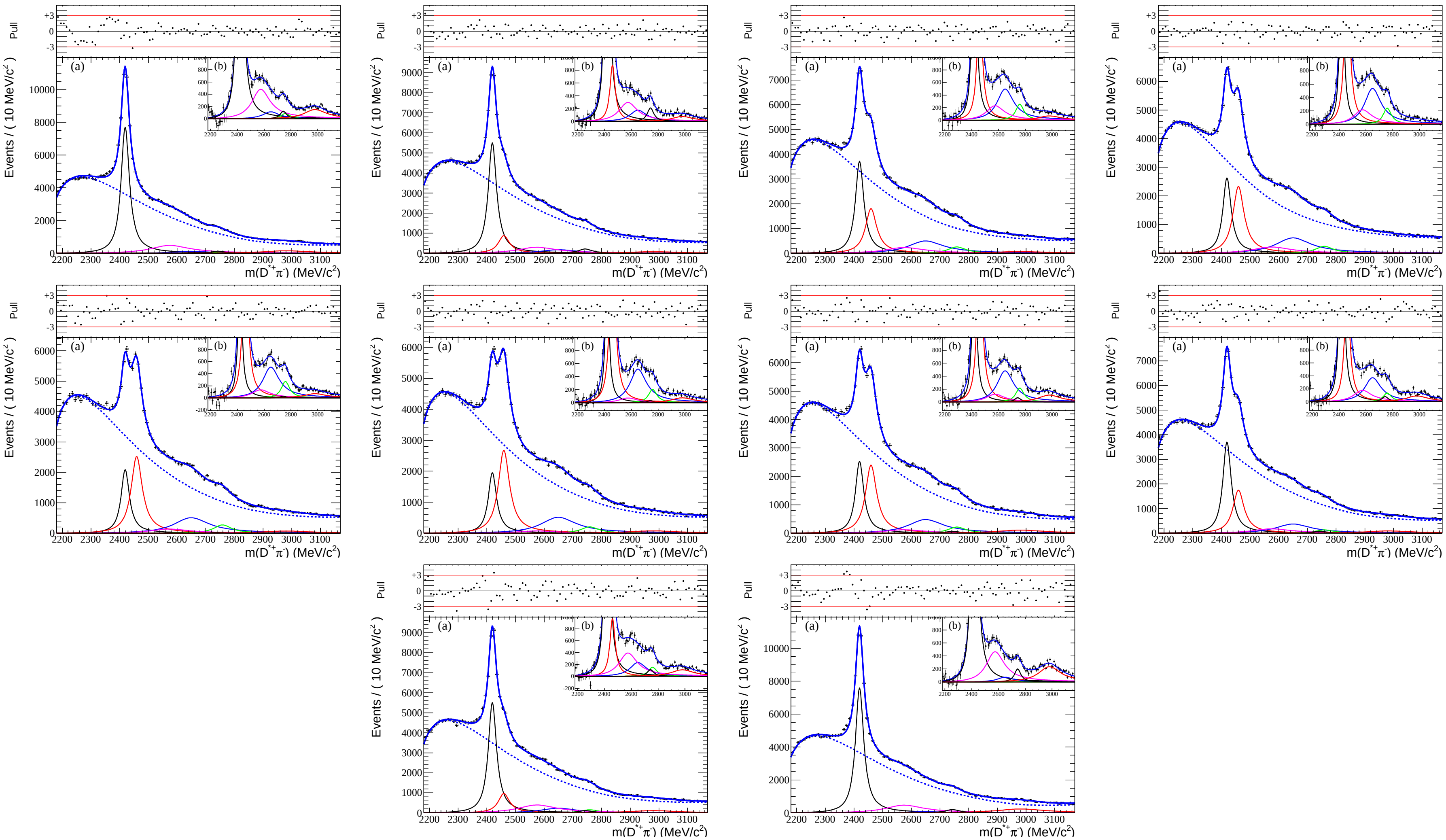

Angular distributions (1).

- Plot yields as functions of $cos\theta_H$ for the different resonances.

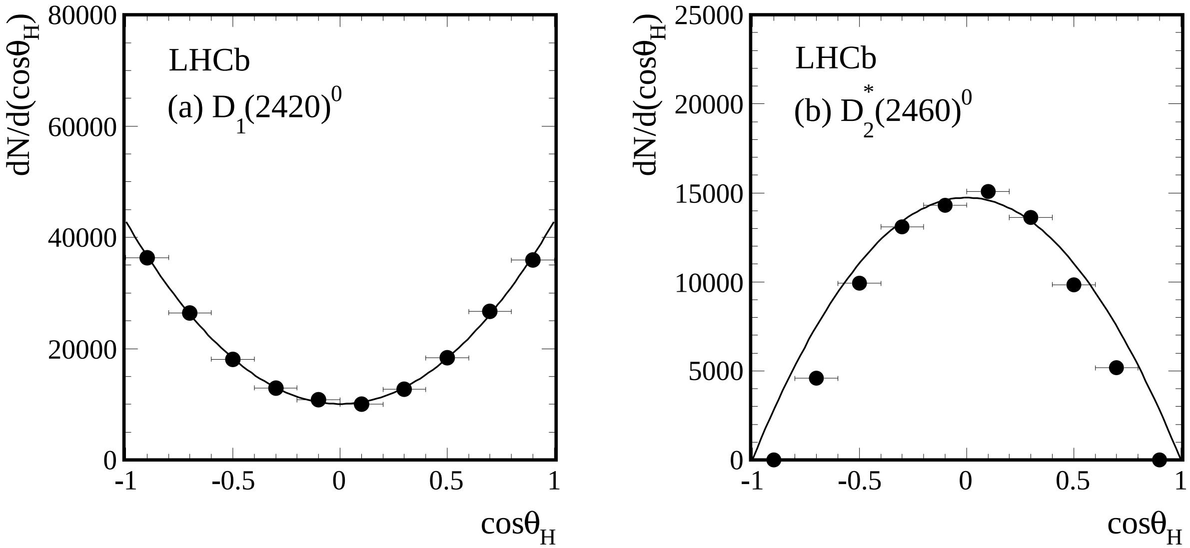

- $D_1(2420)^0$ has $J^P = 1^+$. Fitted with $1 + hcos^2\theta_H$, $h = 3.30 \pm 0.48$. $\chi^2/\mathrm{ndf} = 0.67/8$

- $D_2^*(2460)^0$ has $J^P = 2^+$. Fitted with $sin^2\theta_H$. $\chi^2/\mathrm{ndf} = 8.5/9$

Angular distributions (2).

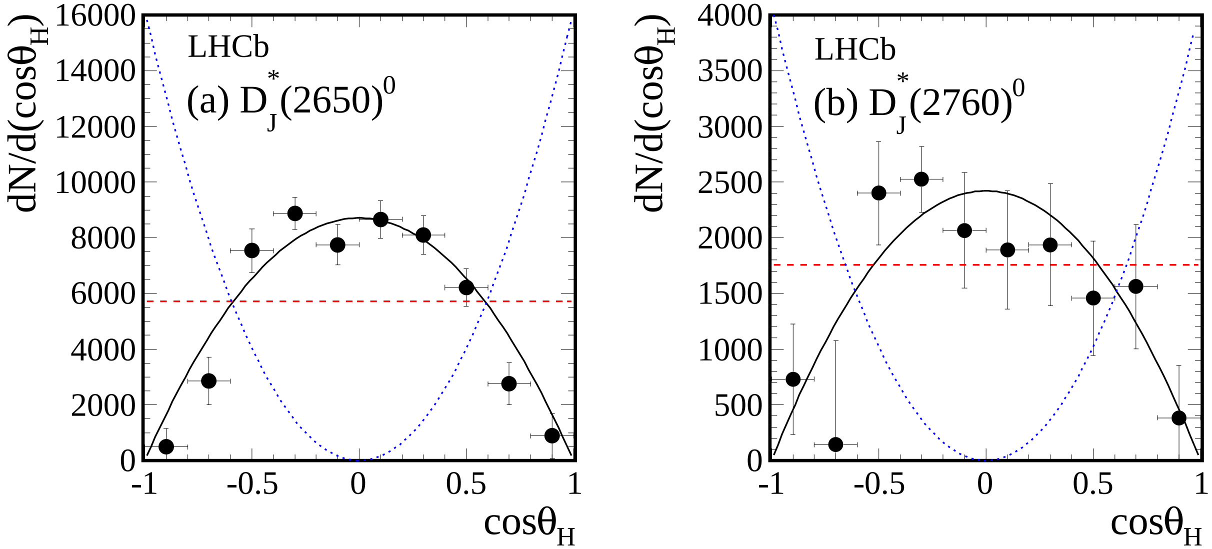

□ $D_J^*(2650)^0$ and $D_J^*(2760)^0$ are consistent with having Natural Parity.

□ Fitted with $sin^2\theta_H$. $\chi^2/\text{ndf} = 6.8/9$ and $\chi^2/\text{ndf} = 5.8/9$ respectively.

(black: natural parity), (dashed red: unnatural parity), (dotted blue: $J^P = 0^-$)

Angular distributions (3).

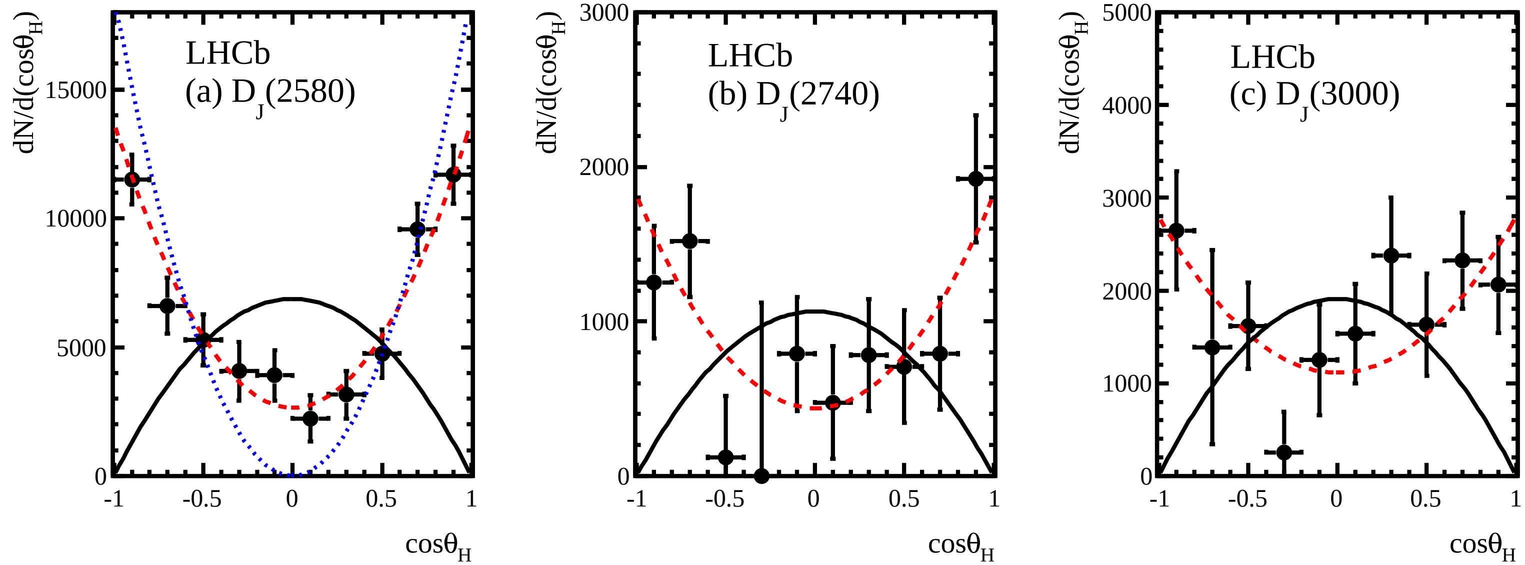

□ $D_J(2580)^0$, $D_J(2740)^0$, and $D_J(3000)^0$ are consistent with having Unnatural Parity. Fitted with $1 + hcos^2\theta_H$.

□ $\chi^2/\text{ndf} = 3.4/8$, $\chi^2/\text{ndf} = 6.6/8$ and $\chi^2/\text{ndf} = 10/8$, respectively.

(black: natural parity), *(dashed red: unnatural parity)*,

(dotted blue: $J^P = 0^-$, $\chi^2/\text{ndf} = 23/9$*)*

Cross-feeds into the $D\pi$ final states.

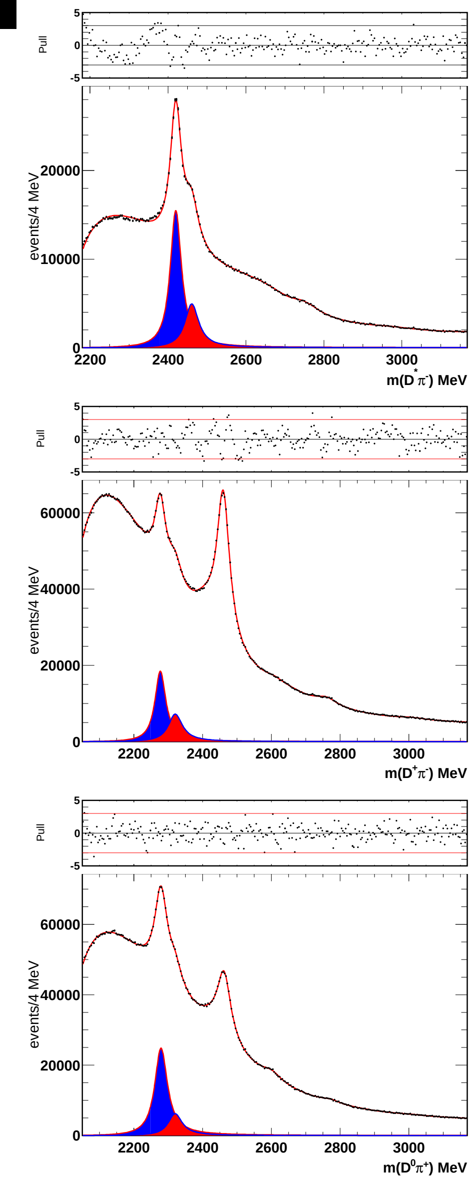

□ We normalize the $D^{*+}\pi^-$ and $D^+\pi^-$ mass spectra using the sum of the $D_1(2420)^0$ and $D_2^*(2460)^0$ signals and obtain:

$$N(D^+\pi^-) = N(D^{*+}\pi^-) \cdot R_{D^+\pi^-}, \qquad R_{D^+\pi^-} = 1.41 \pm 0.02$$

□ Similarly for the $D^0\pi^+$ final state.

$$N(D^0\pi^+) = N(D^{*+}\pi^-) \cdot R_{D^0\pi^+}, \qquad R_{D^0\pi^+} = 1.87 \pm 0.02$$

□ We compute MC cross-feeds into the $D\pi$ from the new resonances observed in the $D^{*+}\pi^-$ mass spectrum using the above normalizations.

Fit to the $D^+\pi^-$ and $D^0\pi^+$ mass spectra.

☐ Cross-feeds (in red) produce a distortion of the $D_2^*(2460)$ and $D_J^*(2650)$ lineshapes.

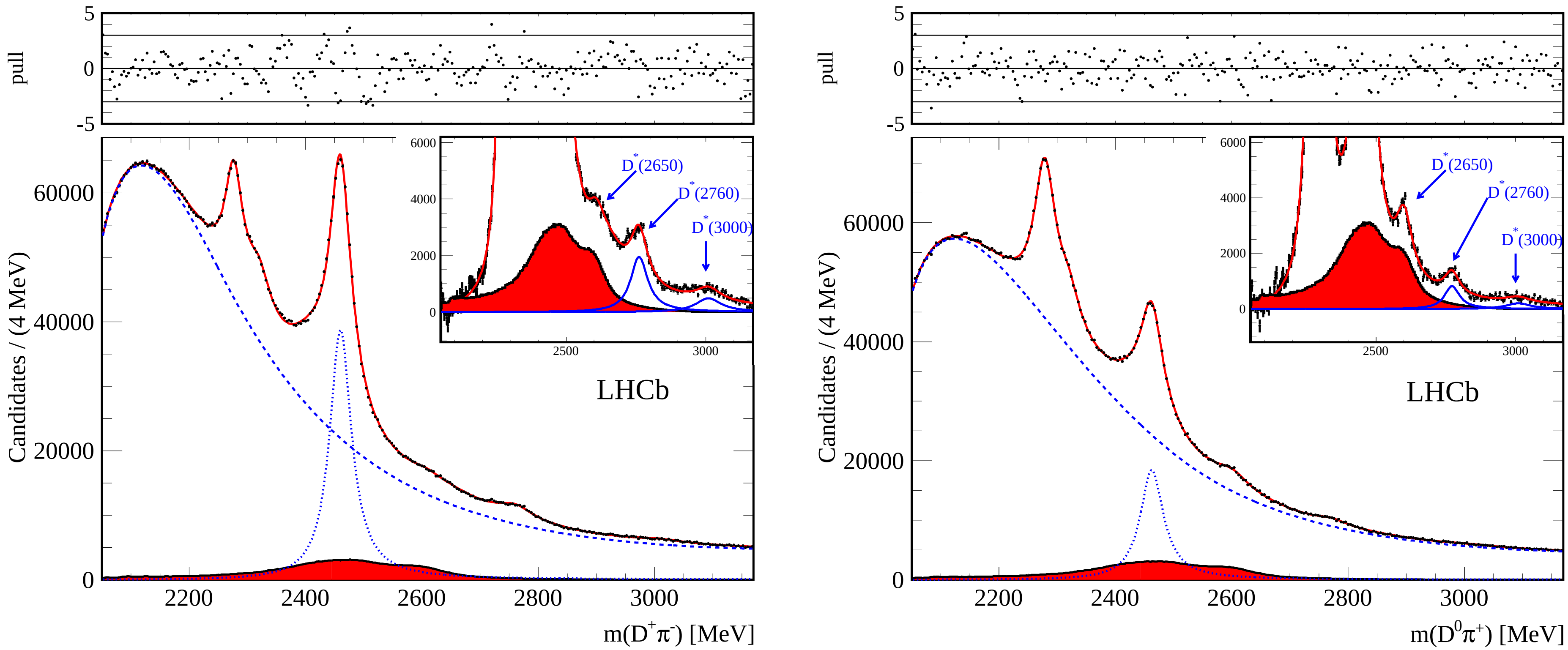

☐ For $D_J^*(2650)$ we rely on the results obtained from the $D^{*+}\pi^-$ mass analysis.

☐ We observe the $D_J^*(2760)$.

☐ The fits requires the presence of a broad structure around 3.0 GeV which we label $D_J^*(3000)$.

Systematic uncertainties.

□ The following systematic uncertainties have been evaluated on the resonances masses and yields.

- The background model has been modified.
- For each mass spectrum we generate and fit 500 new mass spectra with resonances and background yields fixed to the fit results. The background parameters are allowed to vary within $\pm 1\sigma$ from the fitted values.
- In the $D\pi$ mass spectra the simple Breit-Wigner are replaced by relativistic BW.
- Fixed parameters resonances have been relaxed one by one.
- We test, by MC simulations, the possibility of measuring the parameters of the broad $D_0^*(2400)$ in the $D\pi$ final states, with negative results.

Resulting resonances parameters, yields and significances.

Resonance	Final state	Mass (MeV)	Width (MeV)	Yields $\times 10^3$	Sign.
$D_1(2420)^0$	$D^{*+}\pi^-$	$2419.6 \pm 0.1 \pm 0.7$	$35.2 \pm 0.4 \pm 0.9$	$210.2 \pm 1.9 \pm 0.7$	
$D_2^*(2460)^0$	$D^{*+}\pi^-$	$2460.4 \pm 0.4 \pm 1.2$	$43.2 \pm 1.2 \pm 3.0$	$81.9 \pm 1.2 \pm 0.9$	
$D_J^*(2650)^0$	$D^{*+}\pi^-$	$2649.2 \pm 3.5 \pm 3.5$	$140.2 \pm 17.1 \pm 18.6$	$50.7 \pm 2.2 \pm 2.3$	24.5
$D_J^*(2760)^0$	$D^{*+}\pi^-$	$2761.1 \pm 5.1 \pm 6.5$	$74.4 \pm 3.4 \pm 37.0$	$14.4 \pm 1.7 \pm 1.7$	10.2
$D_J(2580)^0$	$D^{*+}\pi^-$	$2579.5 \pm 3.4 \pm 5.5$	$177.5 \pm 17.8 \pm 46.0$	$60.3 \pm 3.1 \pm 3.4$	18.8
$D_J(2740)^0$	$D^{*+}\pi^-$	$2737.0 \pm 3.5 \pm 11.2$	$73.2 \pm 13.4 \pm 25.0$	$7.7 \pm 1.1 \pm 1.2$	7.2
$D_J(3000)^0$	$D^{*+}\pi^-$	2971.8 ± 8.7	188.1 ± 44.8	9.5 ± 1.1	9.0
$D_2^*(2460)^0$	$D^+\pi^-$	$2460.4 \pm 0.1 \pm 0.1$	$45.6 \pm 0.4 \pm 1.1$	$675.0 \pm 9.0 \pm 1.3$	
$D_J^*(2760)^0$	$D^+\pi^-$	$2760.1 \pm 1.1 \pm 3.7$	$74.4 \pm 3.4 \pm 19.1$	$55.8 \pm 1.3 \pm 10.0$	17.3
$D_J^*(3000)^0$	$D^+\pi^-$	3008.1 ± 4.0	110.5 ± 11.5	17.6 ± 1.1	21.2
$D_2^*(2460)^+$	$D^0\pi^+$	$2463.1 \pm 0.2 \pm 0.6$	$48.6 \pm 1.3 \pm 1.9$	$341.6 \pm 22.0 \pm 2.0$	
$D_J^*(2760)^+$	$D^0\pi^+$	$2771.7 \pm 1.7 \pm 3.8$	$66.7 \pm 6.6 \pm 10.5$	$20.1 \pm 2.2 \pm 1.0$	18.8
$D_J^*(3000)^+$	$D^0\pi^+$	3008.1 (fixed)	110.5 (fixed)	7.6 ± 1.2	6.6

□ Significances are evaluated as $\sqrt{\Delta\chi^2}$ where $\Delta\chi^2$ is the difference between the χ^2 values when a resonance is included or excluded from the fit.

□ Significances are all above 5σ.

□ We do not evaluate systematic uncertainties on the parameters of the $D_J^*(3000)/D_J(3000)$ structures because at the edge of the mass spectra.

Discussion (1).

□ The results from this analysis are in fair agreement with BaBar.

□ Some differences on resonances parameters due to a different handling of the cross-feeds.

□ In the present analysis:

- We observe, in the $D^{*+}\pi^-$ mass spectrum, $D_1(2420)^0$ and measure its spin-parity consistent with $J^P = 1^+$.
- We observe, in the $D^{*+}\pi^-$ and $D^+\pi^-$ mass spectra, the $D_2^*(2460)^0$ resonance and find its spin-parity consistent with $J^P = 2^+$.
- We also observe the $D_2^*(2460)^+$ resonance in the $D^0\pi^+$ mass spectrum.

Discussion (2).

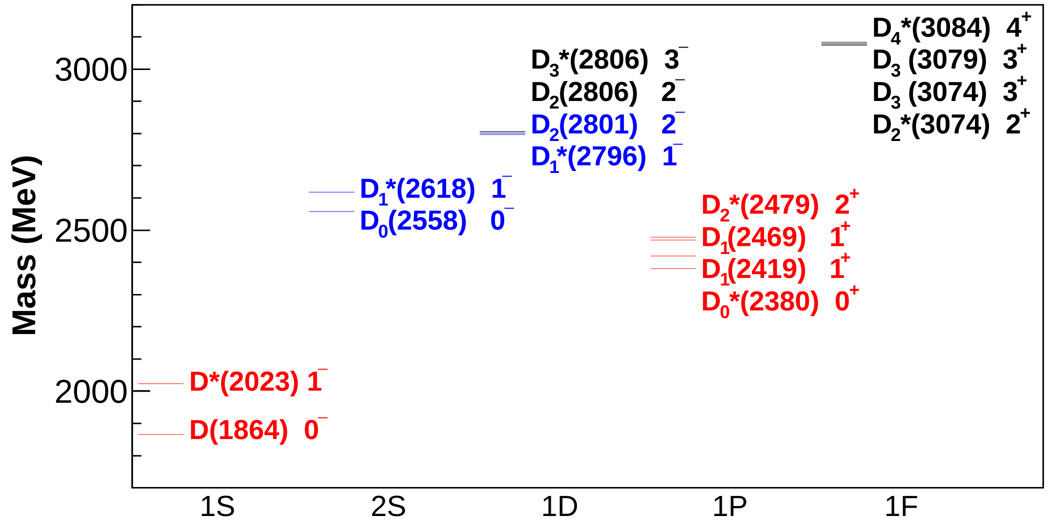

- The $D_J^*(2650)^0$ resonance could be identified as a $J^P = 1^-$ state (2S $D_1^*(2618)$).
- The $D_J^*(2760)^0$ could be identified as a $J^P = 1^-$ state (1D $D_1^*(2796)$).
- The $D_J(2580)^0$ could be identified with the (2S $D_0(2558)$) state, although $J^P = 0^-$ does not fit well the data.
- The $D_J(2740)^0$ could be identified as the $J^P = 2^-$ (1D $D_2(2801)$) resonance.
- Broad structures are observed around 3.0 GeV in the $D^{*+}\pi^-$ and $D\pi$ mass spectra. They could be superpositions of several states.

The D_s states.

□ Masses (in GeV) of charmed meson computed by Godgrey and Isgur.

$c\bar{s}$ $(L=0)$	Mass	$c\bar{s}$ $(L=1)$	Mass	$c\bar{s}$ $(L=2)$	Mass
$D_s(^1S_0)$	1.98	$D_s(^3P_0)$	2.48	$D_s(^3D_1)$	2.90
$D_s(^3S_1)$	2.13	$D_s(^3P_1)$	2.57	$D_s(^3D_3)$	2.92
		$D_s(^3P_2)$	2.59		
		$D_s(^1P_1)$	2.53		

□ Properties of $L=1$ D_{sJ} mesons.

	J^P	Mass (MeV)	Width (MeV)	*Observed/decays*
D_{s0}^*	0^+	2317.8 ± 0.6	< 3.8	$D_s^+\pi^0$
D_{s1}'	1^+	2459.6 ± 0.6	< 3.5	$D_s^{*+}\pi^0, D_s^+\gamma, D_s^+\pi^+\pi^-$
D_{s1}	1^+	2535.12 ± 0.13	0.92 ± 0.05	$D^{*+}K^0, D^{*0}K^+$
D_{s2}^*	2^+	2571.9 ± 0.8	17 ± 4	D^0K^+

□ Mass of the $J^P = 0^+$ and $J^P = 1^+$ expected to be higher than what measured by 120-160 MeV.

Experimental status of the D_s mesons.

□ Experimental status of the D_s mesons.

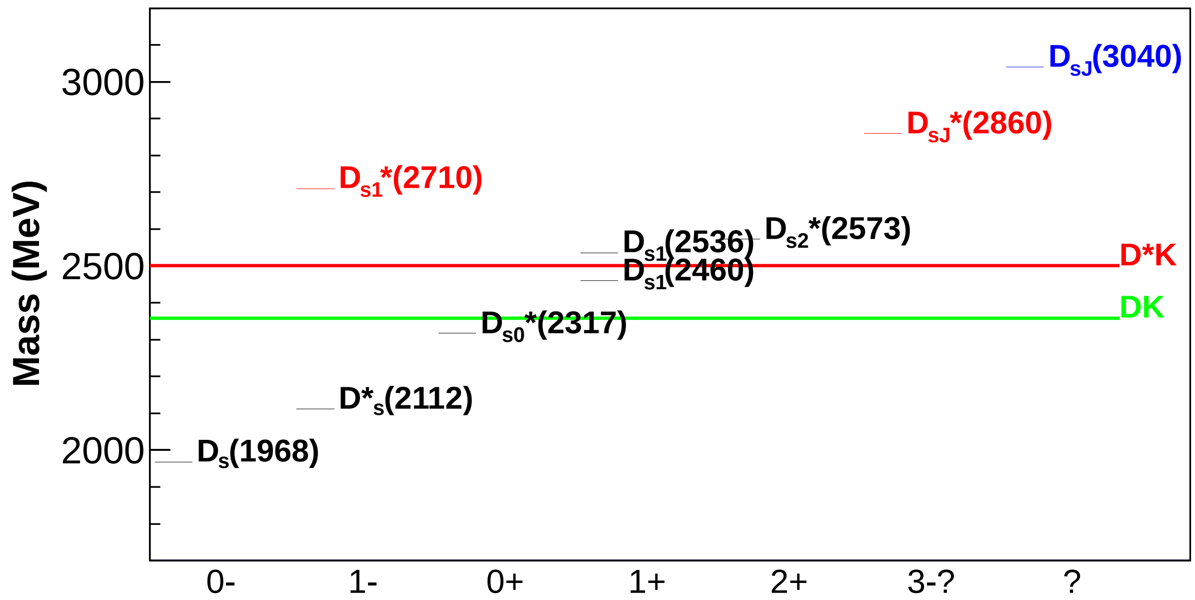

□ Large discrepancy between theory predictions and experiment for $D^*_{s0}(2317)$ and $D_{s1}(2460)$.

□ These two states have masses below the DK and D^*K respectively, therefore very narrow.

The D_s states.

□ BaBar observation of $D^*_{s0}(2317)$ and $D_{s1}(2460)$.

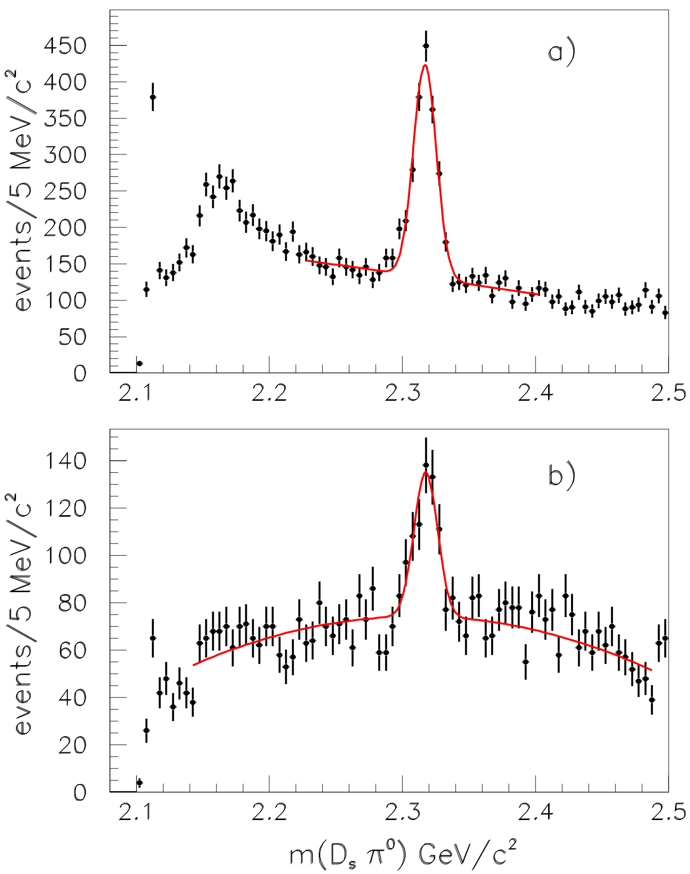

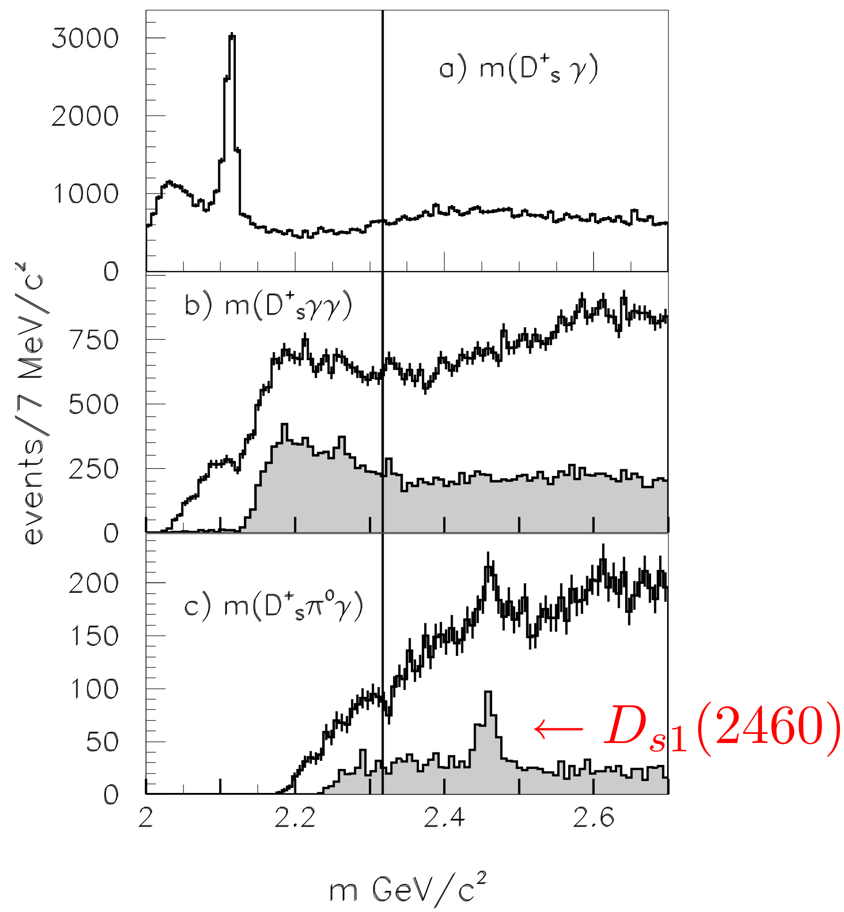

New D_s states observed by BaBar.

□ New states: $D^*_{s1}(2710)$ and $D^*_{sJ}(2860)$ observed by BaBar in the DK and D^*K final states (hep-ex/0607082v3, arXiv:0908.0806v2).

□ A new state: $D_{sJ}(3040)$ observed in the D^*K final state.

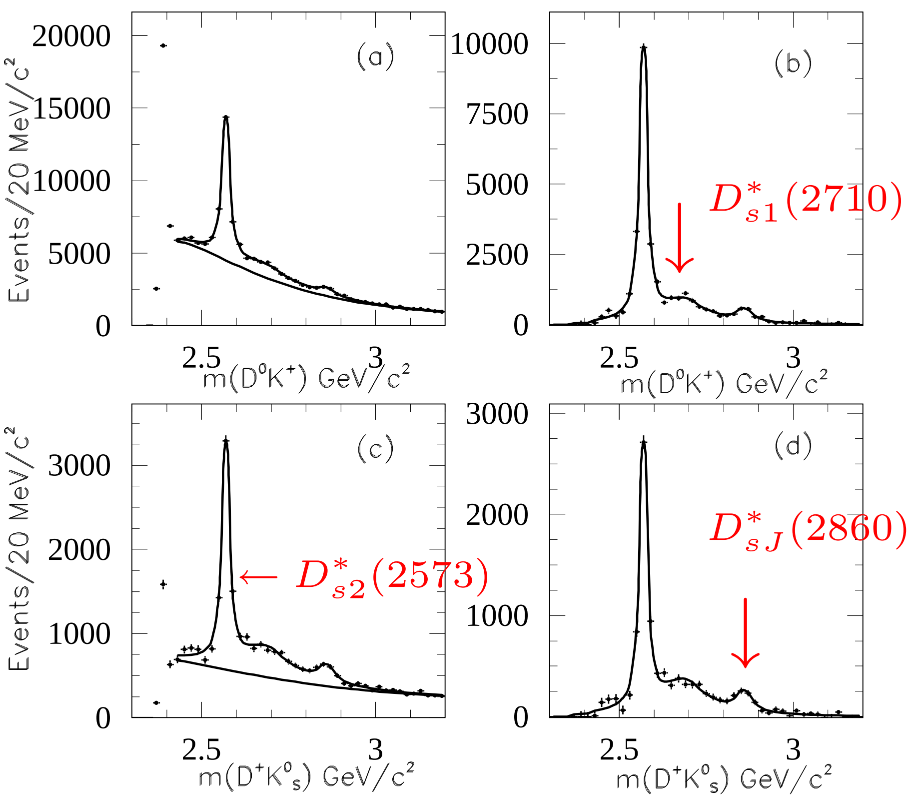

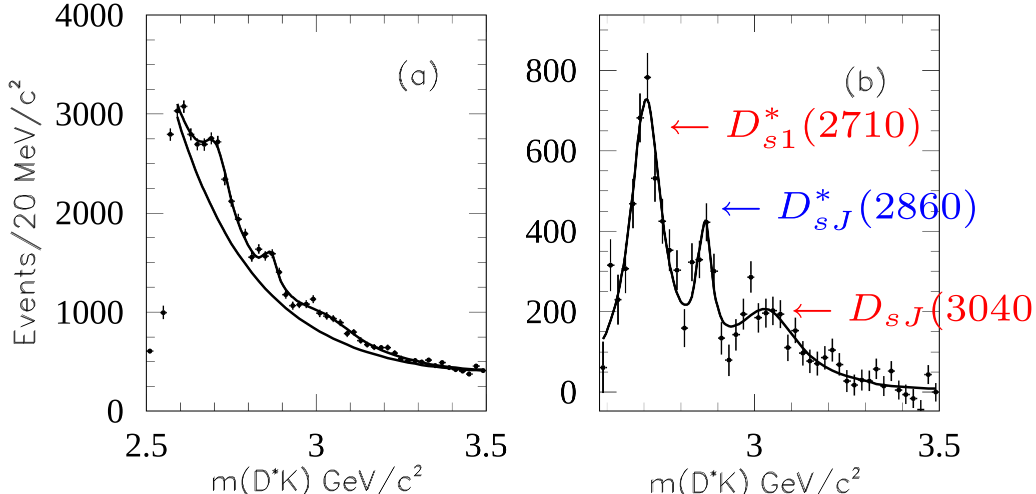

Excited D_s states.

□ Angular distributions. Curves are for natural-parity.

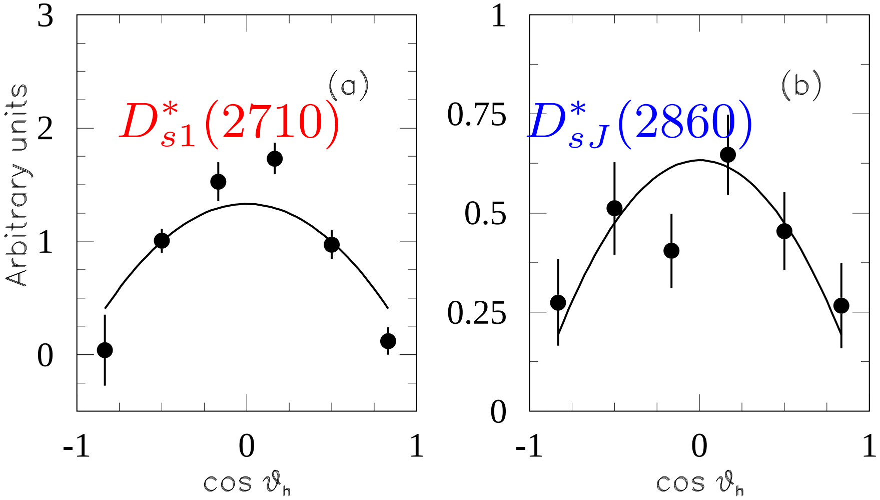

□ BaBar measures the following branching fraction ratios:

$$r = \frac{\mathcal{B}(D^*_{s1}(2710)^+ \to D^* K)}{\mathcal{B}(D^*_{s1}(2710)^+ \to D K)} = 0.91 \pm 0.13 \pm 0.12$$

$$r = \frac{\mathcal{B}(D^*_{sJ}(2860)^+ \to D^* K)}{\mathcal{B}(D^*_{sJ}(2860)^+ \to D K)} = 1.10 \pm 0.15 \pm 0.19$$

Excited D_s states.

□ $D_{s1}^*(2710)$ observed by Belle in a Dalitz plot analysis of $B^+ \to D^0 \bar{D}^0 K^+$ (arXiv:0707.3491).

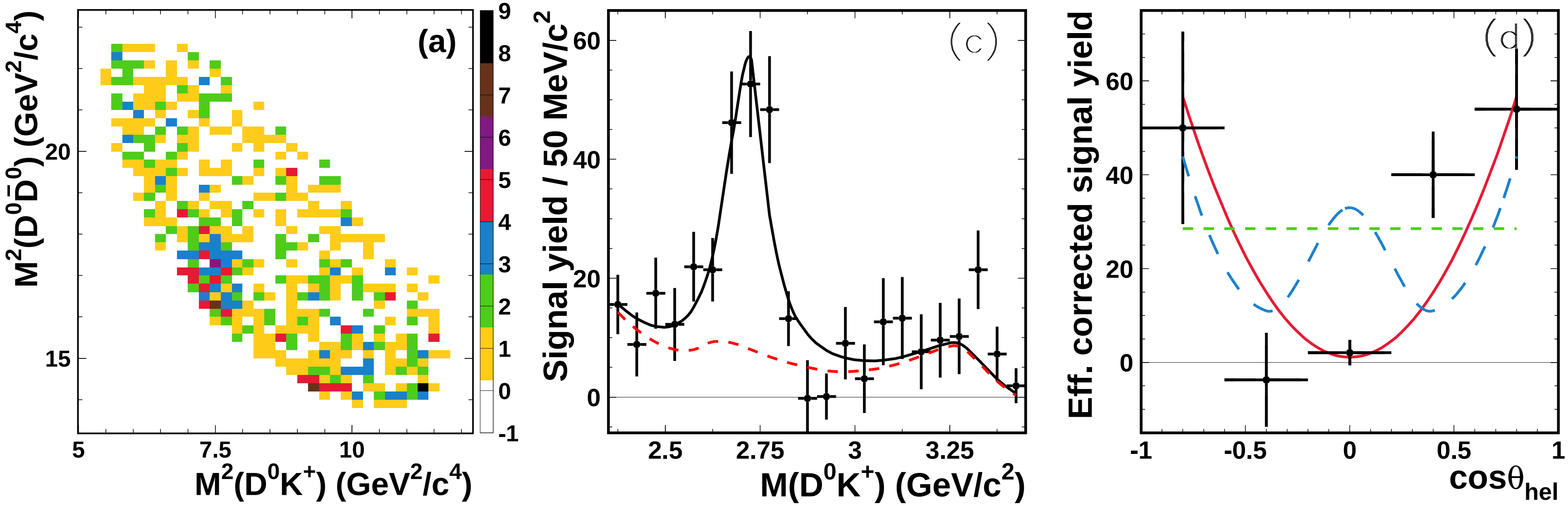

□ $J^P = 1^-$ preferred.

Study of excited D_s states in LHCb.

- We reconstruct the following final states ($1.0\,\mathrm{fb}^{-1}$ of data)(JHEP1210(2012)151):

$$\mathbf{pp} \to \mathbf{X} \quad \mathbf{K^0_S D^+}_{\to K^-\pi^+\pi^+}, \quad \mathbf{pp} \to \mathbf{X} \quad \mathbf{K^+ D^0}_{\to K^-\pi^+}$$

- Similar strategy as in the $D^{(*)}\pi$ analysis.
- Select events with $cos\theta > 0$.
- D^+ and D^0 signals.

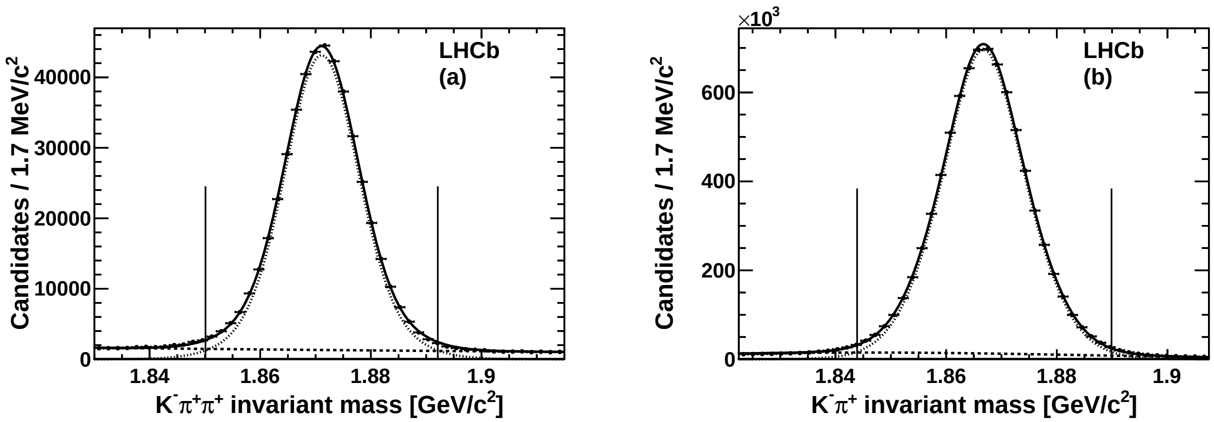

Study of Excited D_s states in LHCb.

□ Two types of K_S^0 signals with different mass resolutions.

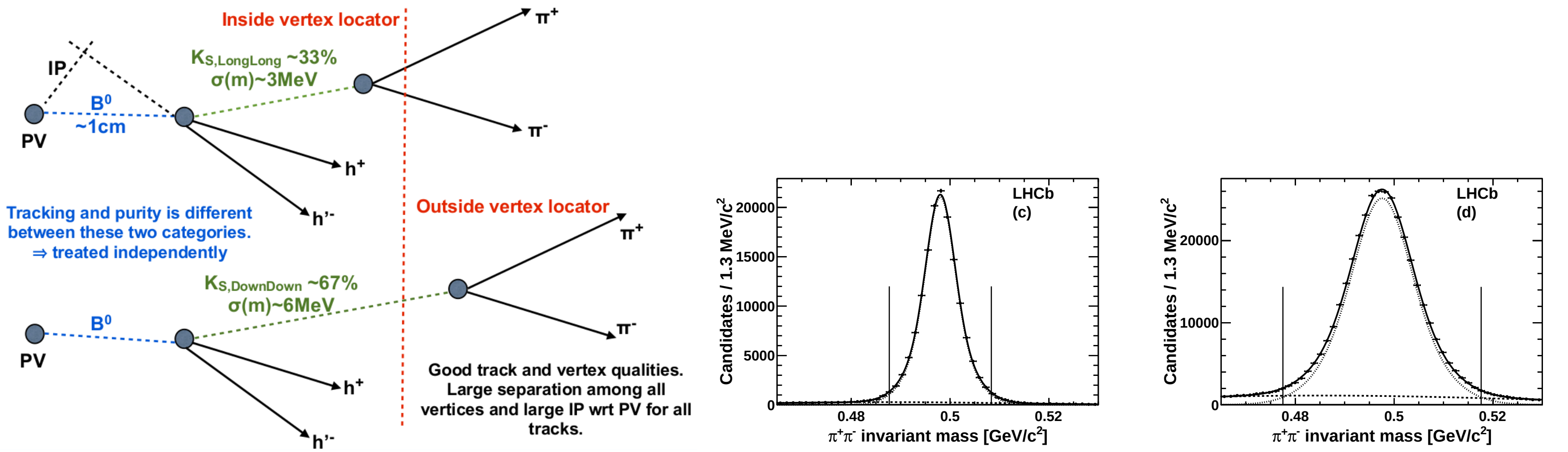

□ Require $cos\alpha$ >0.9999, where α is the angle formed by the K_S^0 vector and the direction defined by the positions of the primary and the meson decay vertex.

□ The pions 3-momenta are added and the K_S^0 energy is computed using the PDG mass.

□ Similar $D^+K_S^0$ mass resolutions($\approx$ 5 MeV) for the two modes.

Study of Excited D_s states in LHCb.

□ Obtain 0.36×10^6 $D^+ K^0_S$ and 3.15×10^6 $D^0 K^+$ candidates.

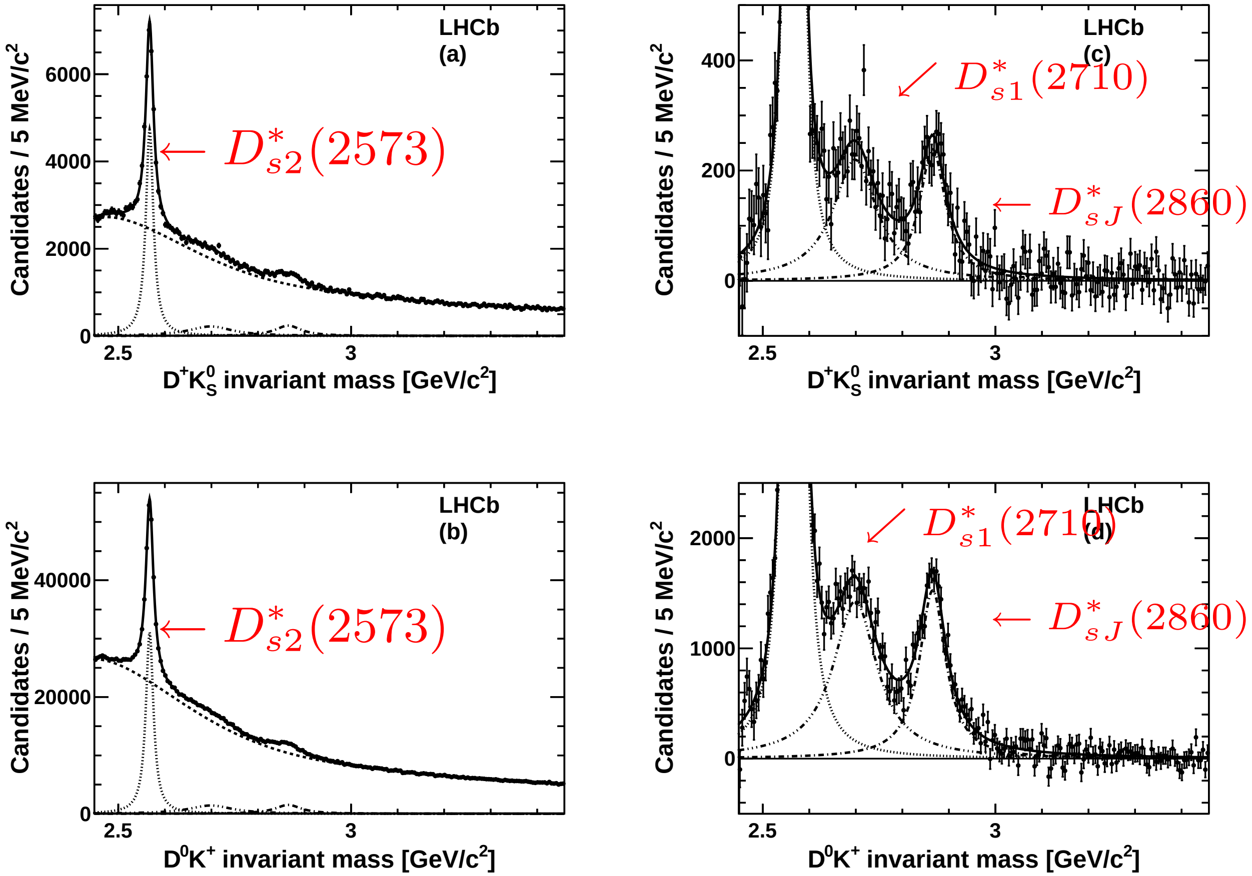

□ First observation of $D^*_{s1}(2710)^+$ and $D^*_{sJ}(2860)^+$ in hadronic collisions.

$D^*_{s1}(2710)^+$ and $D^*_{sJ}(2860)^+$ parameters.

$$
\begin{aligned}
m(D^*_{s1}(2710)^+) &= 2709.2 \pm 1.9(\text{stat}) \pm 4.5(\text{syst})\ \text{MeV}/c^2, \\
\Gamma(D^*_{s1}(2710)^+) &= 115.8 \pm 7.3(\text{stat}) \pm 12.1(\text{syst})\ \text{MeV}/c^2, \\
m(D^*_{sJ}(2860)^+) &= 2866.1 \pm 1.0(\text{stat}) \pm 6.3(\text{syst})\ \text{MeV}/c^2, \\
\Gamma(D^*_{sJ}(2860)^+) &= 69.9 \pm 3.2(\text{stat}) \pm 6.6(\text{syst})\ \text{MeV}/c^2.
\end{aligned}
$$

□ Resonances observed in BaBar and Belle have been confirmed. All results are in agreement.

□ The statistical uncertainties for all parameters are improved by an overall factor of two with respect to the BaBar measurements in the same decay modes.

□ An angular analysis of D^*K samples is needed.

Discussion.

□ We remind that $r = \frac{\mathcal{B}(D_s \to D^* K)}{\mathcal{B}(D_s \to D K)}$

□ (Colangelo et al.(Phys.Rev.D77:014012,2008))
For a $J^P = 1^-$ $D^*_{s1}(2710)$: assuming a radial excitation with l=0 2^3S_1 expects $r(D^*_{s1}(2710)) = 0.91 \pm 0.04$

□ BaBar finds $r(D^*_{s1}(2710)) = 0.93 \pm 0.13_{stat} \pm 0.10_{sys}$,
therefore $D^*_{s1}(2710)$ is likely to be a radial excitation.

□ $J^P = 0^+$ forbidden for $D^* K$, therefore $D^*_{sJ}(2860)$ cannot be a scalar.

□ Colangelo et al.(Phys.Lett.B642:48-52,2006), propose $J^P = 3^-$ assignment.
However the predicted $r(D^*_{sJ}(2860))$ is 0.39, a 3 s.d. difference with respect to the BaBar measurement $r(D^*_{sJ}(2860) = 0.93 \pm 0.13_{stat} \pm 0.10_{sys}$.

□ $D_{sJ}(3050)$ seen in $D^* K$ and not in DK: unnatural parity: $J^P = 0^-, 1^+, 2^-$, ...
Confirmed by the angular analysis.

Discussion

□ Recent calculation of the $c\bar{s}$ spectrum from S. Godfrey and I.T. Jardine (arXiv:1312.6181).

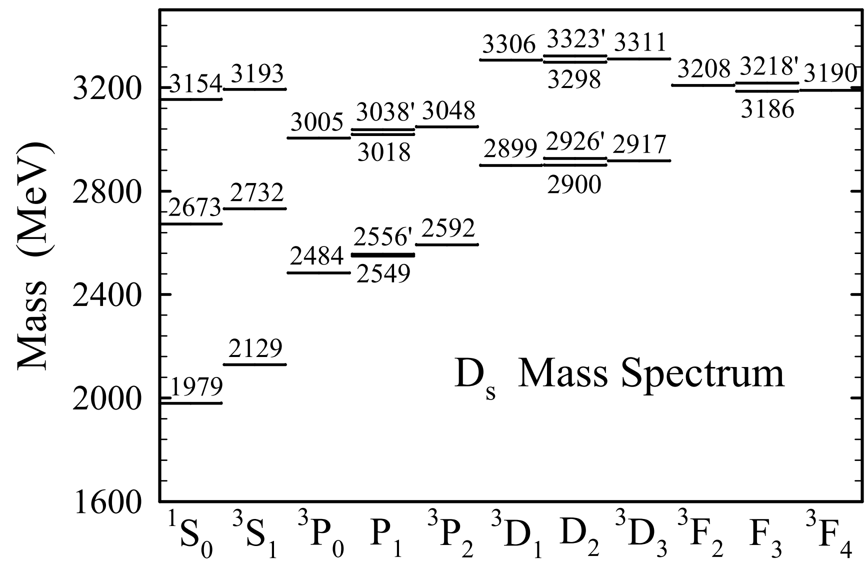

□ See also P. Colangelo et al., arXiv:1207.6940.

□ Expect several other states in this mass region.

□ It is possible that more than one state is contributing in both $D^*_{s1}(2710)$ and $D^*_{sJ}(2860)$ mass regions.

□ The possible existence of charm-strange hadronic molecules has been proposed (F. Guo et al.arXiv:1403.4032).

Summary and outlook.

□ Charm spectroscopy has made important progress at LHCb.

□ In the sector of the D_J spectroscopy we observe two new natural parity and two new unnatural parity resonances to be compared with previous measurements from BaBar.

□ We also observe further structures in the 3000 MeV mass region.

□ In the sector of the D_{sJ} spectroscopy we confirm, with higher statistics, results obtained at B factories and therefore $D^*_{s1}(2710)$ and $D^*_{sJ}(2860)$ are now "established".

□ Other analyses are in progress, in particular the study of the $D^{*+}K^0_S$ system. A trigger line is being built for this channel.

□ In the near future, we expect new results from the study of B and B_s decays.

□ In these exclusive decays will be possible to perform spin analysis and measurements of branching fractions.

Backup.

Fits quality, cross checks and systematic uncertainties

- Summary of the fits to the different mass spectra.

Final state	Selection	Fit Range (MeV)	Number of bins	Candidates ($\times 10^6$)	χ^2/ndf
$D^+\pi^-$	Total	2050-3170	280	7.90	551/261
$D^0\pi^+$	Total	2050-3170	280	7.50	351/262
$D^{*+}\pi^-$	Total	2180-3170	247	2.04	438/234
$D^{*+}\pi^-$	*Natural parity sample*			0.98	263/229
$D^{*+}\pi^-$	*Unnatural parity sample*			1.06	364/234
$D^{*+}\pi^-$	*Enhanced unnatural parity sample*			0.55	317/230

- Cross checks on the fits results and stability have been performed.
  - The p_T cut has been lowered to 7.0 GeV/c: results are in agreement within the statistical errors.
  - For each mass spectrum we generate and fit 500 new mass spectra obtained by Poisson fluctuations of each bin content.
- The following systematic uncertainties have been evaluated on the resonances masses and yields.
  - We make use of different background models.
  - For each mass spectrum we generate and fit 500 new mass spectra with resonances and background yields fixed to the fit results. The background parameters are allowed to vary within $\pm 3\sigma$ from the fitted values.
  - In the $D\pi$ mass spectra the simple Breit-Wigner are replaced by relativistic BW.
  - Fixed parameters resonances have been relaxed one by one.